Equivalent Capacity in Carrier Aggregation-Based LTE-A Systems: A Probabilistic Analysis

Ran Zhang, *Student Member, IEEE*, Zhongming Zheng, *Student Member, IEEE*, Miao Wang, *Student Member, IEEE*, Xuemin (Sherman) Shen, *Fellow, IEEE*, and Liang-Liang Xie, *Senior Member, IEEE*

Abstract—In this paper, we analyze the user accommodation capabilities of LTE-A systems with carrier aggregation for the LTE users and LTE-A users, respectively. The adopted performance metric is *equivalent capacity* (EC), defined as the maximum number of users allowed in the system given the user QoS requirements. Specifically, both LTE and LTE-A users are divided into heterogeneous user classes with different QoS requirements, traffic characteristics and bandwidth weights. Two bandwidth allocation strategies are studied, i.e., the fixed-weight strategy and the cognitive-weight strategy, where the bandwidth weights of different user classes are prefixed under the former and dynamically changing with the cell load conditions under the latter. For each strategy, closed-form expressions of ECs of different user classes are derived for LTE and LTE-A users, respectively. A net-profit-maximization problem is further formulated to discuss the tradeoff among the bandwidth weights. Extensive simulations are conducted to corroborate our analytical results, and demonstrate an interesting discovery that only a slightly higher spectrum utilization of LTE-A users than LTE users can result in a significant EC gain when the user traffic is bursty. Moreover, the cognitive-weight strategy is shown to outperform considerably the fixed-weight one due to stronger adaptability to the cell load conditions.

Index Terms—LTE-A systems, carrier aggregation, admission control, equivalent capacity, QoS provisioning.

I. INTRODUCTION

IN order to meet the fulminic growth of the high-data-rate aspiration, the 3rd Generation Partnership Project (3GPP) has proposed the Long Term Evolution-Advanced (LTE-A) [1] as the 4G mobile communication standard, providing substantial improvements over its original LTE standard [2]. Specifically, LTE-A could achieve 1 Gbps peak data rate for downlink and 500 Mbps for uplink with a maximum 100 MHz bandwidth, respectively, compared with 300 Mbps and 75 Mbps with up to 20 MHz bandwidth under LTE; besides, LTE-A standard has higher spectral efficiency, stronger intercell interference control and supports the coexistence of multi-tier cells [3] by integrating several advanced techniques. As one of the

most momentous techniques in LTE-A, Carrier Aggregation (CA) allows scalable bandwidth extension via aggregating multiple smaller band segments, each called a Component Carrier (CC), into a wider virtual frequency band to transmit at higher rates [4]. With the backward compatibility of LTE-A, both the legacy LTE users and LTE-A users can operate under CA-based LTE-A systems, where LTE users can use only one CC while LTE-A users can enjoy concurrent multi-CC transmissions exploiting CA.

While LTE-A is attracting considerable attention, the industry is busy with its realization, which not only covers prototype design of the cellphone chipsets [5], but also expands LTE-A into many new areas, such as LTE-A in unlicensed spectrum [6], direct device-to-device [7], vehicular communications [8], [9], etc. Many research issues emerge in the realization process of LTE-A, among which Resource Management (RM) is indispensable in optimizing the network resource utilization. Since LTE-A adopts Orthogonal Frequency Division Multiple Access (OFDMA) as the downlink access technology [10], RM in LTE-A systems can date back to that in OFDMA networks [11]–[13], where the subcarrier allocation and power management problems are fully analyzed. However, due to the unique features of the new standard, these works may not be directly applicable to LTE-A systems. For instance, different from subcarriers in OFDMA networks, the minimum bandwidth allocation unit in LTE-A is Physical Resource Block (PRB) [10], composed of 12 continuous subcarriers; besides, as CA allows cross-CC load balancing and scheduling [14], new methods are required to further improve the overall resource utilization.

Recently, many works have been done to incorporate the unique characteristics of LTE-A into the design RM strategies, aiming to improve the throughput [14], [15], enhance the energy efficiency [16], mitigate the intercell interference [17], etc. Most of the works so far conduct evaluations based on the user-centric performance, e.g., average user throughput. The theoretical analysis on the system-centric limiting capabilities is still embryonic, which, however, can serve as essential benchmarks for system stability maintenance and Quality of Service (QoS) guarantee. In this paper, we explore the downlink admission control process in a CA-based LTE-A system and analyze its user accommodation capabilities for the legacy LTE and LTE-A users, respectively. Specifically, both the LTE and LTE-A users are divided into heterogeneous classes with different QoS requirements (i.e., throughput and loss probability requirements) and traffic descriptors (i.e., active probabilities) as defined in Section III-B. Each user class is allocated with a bandwidth weight. Two bandwidth allocation strategies are

studied, namely the fixed-weight strategy and the cognitive-weight strategy, where the bandwidth weights of different classes are pre-fixed in the former while can be dynamically changed in the latter according to the instantaneous load conditions of different classes. The adopted performance metric is *equivalent capacity* (EC) [18], referring to the maximum number of users of each class that can be admitted into the system based on the QoS requirements.

To properly determine the EC in LTE-A systems, the following challenges should be deliberated. First, unlike the wired networks, the channel conditions of the wireless mobile environment are dramatically time-fluctuating due to the complicated propagation environment. Consequently, the assigned bandwidth to satisfy the minimum throughput requirement of a user changes from time to time, making it difficult to determine the EC based on the user throughput requirements. Second, based on the statistics of user traffic, how to determine the EC of each class to satisfy the loss probability requirements under different bandwidth allocation strategies is a challenging issue. Third, as LTE-A users can transmit with CA, whether the LTE-A users can benefit much from CA over the LTE users needs to be justified. Last but not least, since heterogeneous user classes coexist, the tradeoff among the bandwidth allocation weights for different classes and the criteria therein should be carefully discussed. Revolving around these challenges, the contributions of this paper are fivefold.

- We take advantage of the concept *effective bandwidth* [19] to map the minimum required throughput of each user class to a unified bandwidth, considering the multi-cell co-channel interference. With the derived bandwidth, users are provided with probabilistic QoS guarantee, which means that instead of guaranteeing the QoS by 100%, the system allows the QoS requirement to be violated with a very small probability.
- A simple yet effective on-off model is applied to depict the per-user traffic generation, based on which the aggregate traffic generation of each user class is modeled as a birth-death random process.
- Under each bandwidth allocation strategy, closed-form expressions of ECs are deduced first for a single-CC LTE-A system leveraging the binomial-normal approximation. The result is then extended to LTE-A systems with multiple CCs, where the ECs between LTE and LTE-A users are compared.
- The tradeoff between the bandwidth weights of different user classes is evaluated via a net-profit-maximization problem for both LTE and LTE-A users under both bandwidth allocation strategies, considering the operator service profits, user satisfaction and instantaneous traffic load conditions.
- Extensive simulation results are provided to validate our theoretical analysis and compare the EC performance between LTE and LTE-A users and between two bandwidth allocation strategies. The optimal net-profits under two bandwidth allocation strategies are also compared.

To the best of our knowledge, this is the first work in literature that gives theoretical analysis on the admission control process in CA-based LTE-A systems. The research outcomes should shed some light not only on theoretically quantifying the benefits of CA but also on benchmarking the QoS-aware admissible region for heterogeneous user classes in the admission control process of CA.

The remainder of this paper is organized as follows. Section II surveys the related works and Section III describes the system model. Sections IV and V present the theoretical analysis of the closed-form relationship under the fixed-weight strategy and cognitive-weight strategy, respectively. The tradeoff among bandwidth weights of different user classes is evaluated in Section VI. Extensive simulation results are given in Section VII. Finally, Section VIII concludes the paper.

II. RELATED WORKS

In this section, we review the related works on LTE-A RM and the concept of effective bandwidth.

A. RM in LTE-A Systems

RM in LTE-A systems can be traced to the works on RM in OFDMA networks, where previous studies [11]–[13] mainly focus on reorganizing the limited network resources to optimize the network performance. In [11], a novel scheme for the allocation of subcarriers, rates, and power was proposed to maximize the aggregated data rates. In [12], the energy efficiency problem was investigated for cognitive radio systems under the QoS constraints. In [13], the uplink relay selection problem was discussed to enhance the total achievable throughput under total power constraint. Different from OFDMA networks, RM in LTE systems has some new challenges. For instance, since the minimum bandwidth allocation unit in LTE is the PRB, [20] put forward a distributed and coordinated PRB and power allocation scheme to mitigate the intercell interference in LTE. As the control channel structure is updated in LTE over OFDMA systems, [21] showed different conditions when an LTE system is data-channel limited or control-channel limited. [22] further gave a comprehensive overview of downlink RM for LTE systems.

As one of the most promising technologies adopted in LTE-A systems, CA provides the opportunities for cross-CC load balancing and scheduling. References [14]–[17] studied the benefits of CA from different perspectives. In [14], a joint carrier load balancing and cross-CC packet scheduling scheme was presented, which compared the average and cell-edge throughput between LTE and LTE-A users. In [15], the average user throughput was compared between N separate LTE carriers and N aggregated LTE-A CCs. In [16], uplink cross-layer carrier selection and power control problems were investigated, aiming to improve the average user throughput with the power offset effects. In [17], a novel intercell interference control scheme, called ACCS, was proposed, where femtocells adaptively choose CC subsets for interference mitigation. However, most of the existing works evaluate the system performance based on the metric—average throughput, without comprehensive analysis on the system limiting capabilities. Our previous work [23] studied the system-level user accommodation

capabilities for heterogeneous user classes based on the metric—EC, but the characteristics of the wireless physical channel is not involved into the analysis. Besides, the bandwidth weights for different classes were assumed to be fixed and no discussion about the tradeoff among the weights was given. In this work, we focus on EC performance of LTE-A systems with CA considering both fixed and dynamically changing bandwidth weights under the wireless fading statistics. In addition, a net-profit-maximization problem is formulated to discuss the tradeoff for both LTE and LTE-A users under different bandwidth allocation strategies.

B. The Effective Bandwidth Concept

The effective bandwidth concept was first proposed in [24], where Elwalid et al. initiated the concept by assigning a unified notional bandwidth to each connection with identical grade of service and traffic characteristics to control the buffer overflow probability. In [25], Chang et al. provided a simple intuitive derivation of the effective bandwidth by using large deviation theory and the Laplace integration method. In [19], Wu et al. took a step further by incorporating the wireless channel statistics into the derivation framework and studied the wireless link-level delay bound by employing the dual of the effective bandwidth—effective capacity. In [26], Abdrabou et al. applied the results of [19] to model the probabilistic packet delivery delay in vehicular ad hoc networks. In this paper, we apply the concept to an LTE-A system to evaluate its EC performance. Considering the wireless multi-cell co-channel interference, unified effective bandwidth is derived while keeping the violation probability of the minimum throughput requirement under a small level. Based on the effective bandwidth, closed-form expressions of EC can be deduced.

III. SYSTEM MODEL

We consider a multi-cell downlink scenario where the base stations (BSs) are deployed following a homogeneous Poisson point process (PPP) [27] with density measure λ_{BS}, i.e., the number of BSs within any given region A with area $|A|$ is a Poisson random variable with parameter $\lambda_{BS}|A|$, and the BSs are uniformly located within A. Denote all the BSs as a set Φ_{BS}. The users are uniformly distributed within region A. Each user will be associated to its nearest BS for service. Under such an association policy, the actual coverage area of a BS becomes a Voronoi cell [28] where any point in a Voronoi cell has a shorter distance to the corresponding BS than to other BSs, as shown in Fig. 1. LTE-A and LTE users are considered for the analysis, respectively. Both LTE and LTE-A users are divided into K classes with different QoS requirements (i.e., the throughput and loss probability requirements) and traffic descriptors (i.e., active probabilities). For each class-k user, the minimum required throughput is r_k^u and the maximum loss probability is δ_k. δ_k refers to the maximum probability that there exist class-k users which are admitted into the system but cannot get any bandwidth when they turn active, i.e., having packets to deliver. The important symbols are summarized in Table I.
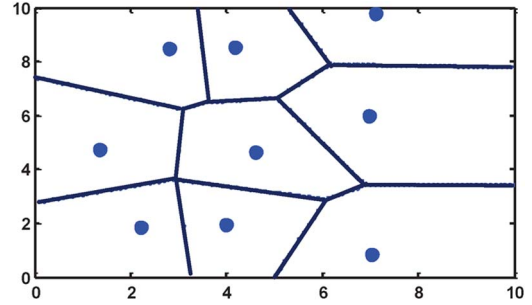

Fig. 1. The Voronoi cells formed by 9 BSs uniformly located within a 10 km × 10 km area.

TABLE I
SUMMARY OF IMPORTANT MATHEMATICAL NOTATIONS

Symbol	Definitions
λ_{BS}	The density measure of BSs in the considered area A
Φ_{BS}	The set of BSs in the considered area A
α_k, β_k	The state transition rates of the on-off Markov traffic model
B_l^{cc}	The channel bandwidth of lth CC
$B_{lk}^{cc(,nor)}$	The (normalized) bandwidth assigned to user class k in lth CC
B_k^u	The effective bandwidth assigned to each class-k user
$B_k^{u,ins}(t)$	The instantaneous required bandwidth to satisfy r_k^u at time t when the channel gain is $h_k^{u,ins}(t)$
δ_k^u	The maximum loss probability of user class k
K	The total number of user classes in the system
N_{lk}	The equivalent capacity (EC) of user class k in CC l
$N_k^{LTE(-A)}$	The total EC of user class k when LTE (LTE-A) users are considered
N_{l1}^{ad}	The current number of admitted class-1 users in CC l
n_{lk}	The number of class-k users currently being served in lth CC
p_k	The active probability of user class k
π_{ik}	The steady-state probability of the state i of the composite birth-death process for user class k
r_k^u	The minimum throughput requirement of user class k
Γ_k	A constant which varies with δ_k
σ_{lk}	The standard derivation of the number of active class-k users in lth CC when N_{lk} class-k users are admitted
$S_{o,lk}$	The overload state in and beyond which the loss occurs for user class k in lth CC
ω_{lk} (ω_{lk}^{max})	The (maximum) bandwidth weight of class k in CC l

A. CC Bandwidth Structure

We first present the CC bandwidth structure in LTE-A systems. As shown in Fig. 2, the channel bandwidth B_l^{cc} of the lth CC is up to 20 MHz and contains two parts: the guard bands (GBs) and the transmission bandwidth. As specified in [29], the GBs are set on both sides of each CC to avoid interference caused by Doppler Shift and Frequency Aliasing Effect in real systems [30]. No effective data will be transmitted in the GBs. The total percentage of GBs is denoted as θ. For the lth CC, the transmission bandwidth is divided into P_l PRBs, each composed of N_l^{sc} continuous subcarriers with bandwidth B_l^{sc}. The relationship of all the above variables is given as

$$P_l = \frac{(1-\theta)B_l^{cc}}{B_l^{sc} N_l^{sc}}, \quad l = 1, 2, \ldots, n, \tag{1}$$

where n denotes the number of CCs. The assignment of PRBs for each user is determined according to the throughput requirement and channel conditions. The interference from other users
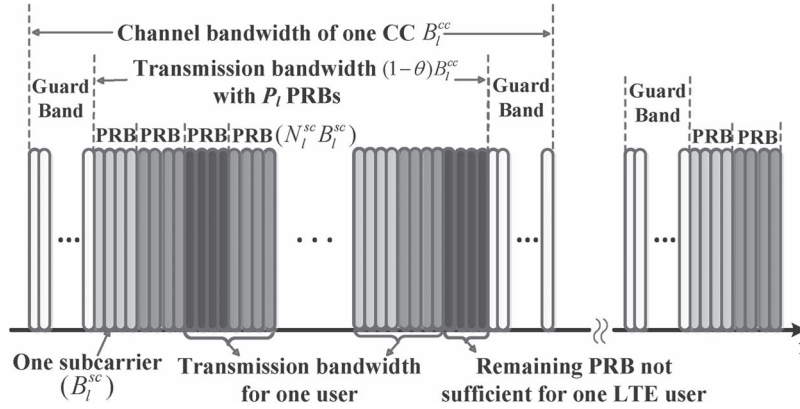
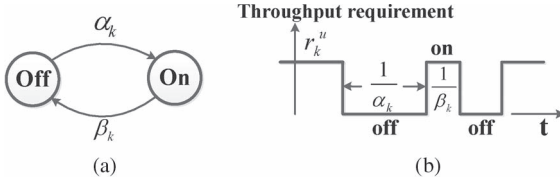Fig. 2.   Bandwidth structure for LTE-A systems based on OFDMA.

Fig. 3.   On–Off traffic generation model of one user.

in the same cell is ignorable due to the orthogonality of PRBs. For LTE users, the transmission bandwidth may not be fully utilized as the remaining PRBs in one CC may not be sufficient to serve any more users. However, for LTE-A users, these unused PRBs in different CCs could be combined together to jointly serve a user through the CA technique. In this way, the LTE-A users could achieve higher spectrum usage than the LTE users. In this paper, such PRBs are referred to as *semi-usage PRBs*.

B. Traffic Generating Model

We consider both voice sources and video sources. Two traffic models which are corroborated by empirical data [31], [32] are exploited, respectively. For the voice sources, we use an on-off traffic source model to describe the dynamics of the user traffic [31]. Each voice source is represented by a two-state continuous-time Markov chain. with the states *on* and *off*, as depicted in Fig. 3(a). The state *on* means the user is active and requires a minimum throughput of r_k^u for class-k users, while the user remains silent in the state *off*. The *on* and *off* intervals are exponential with transition rates denoted as β_k and α_k, respectively. Then the average *on* and *off* period are $1/\beta_k$ and $1/\alpha_k$ as shown in Fig. 3(b)). Therefore, the average probability that a class-k user is on (denoted as active probability p_k) can be calculated as,

$$p_k = \frac{1/\beta_k}{1/\alpha_k + 1/\beta_k} = \frac{\alpha_k}{\alpha_k + \beta_k}, \quad k = 1, 2, \ldots, K. \quad (2)$$

Notice that we consider bursty users satisfying $p_k \ll 1$, e.g., the average *on* period is far smaller than the average *off* period.

Unlike the constant data rate generated by voice sources, one video source has time-varying data rate which cannot be simply modeled as an on-off model. However, according to [32], one class-k video source can be effectively modeled as $M_k (M \gg 1)$ independent and statistically multiplexed mini-sources with identical constant data rate r_k^{mini}. Each mini-

source can be modeled with the above on-off model. Therefore, when the video sources are considered, the equivalent mini-sources can be treated in a similar way with the voice sources, except that the EC for the mini-sources of the same video user class should be a multiple of M_k. As the main emphasis of this paper lies in the EC comparison between LTE and LTE-A users, we only use voice sources in the following analysis for the simplicity of computation and presentation.

C. Bandwidth Sharing Model

For bandwidth allocation among different user classes, two strategies are considered, i.e., fixed-weight strategy and cognitive-weight strategy. Under the former strategy, the bandwidth allocation weights ω_{lk} for class-k users are pre-fixed; while under the latter one, the weights can dynamically change with the instantaneous number of active users of each class. Moreover, in the latter strategy, different user classes are endowed with different priorities. Preemptive priority is considered with which the services of some lower-priority users will be interrupted by the higher-priority users when there is no available bandwidth. Thus, the loss probability of one user class is merely affected by the number of users with higher priorities. Without loss of generality, the priorities are set in a descending order with respect to k. In addition, to avoid the spectrum monopoly and evaluate the impact of user dissatisfaction factor on ECs, a maximal bandwidth allocation weight $\omega_{lk}^{\max}$ is set for each class in the latter strategy. One important application scenario of the latter strategy is the bandwidth allocation for user classes with diverse delay requirements, where the user class with more strict delay requirement will be assigned with higher priority.

For spectrum sharing within one user class, random spectrum access (RSA) method is used. In each transmission time slot, if there are not enough PRBs for every active user in one class, the system randomly chooses a subset of active users to schedule. One scheduled user is randomly assigned with several PRBs according to its QoS requirements. One LTE user can only be assigned with PRBs within one CC; while one LTE-A user can be assigned with PRBs from different CCs. Transmission buffers are not considered here, thus, the packets that are generated in one slot but cannot be transmitted within the same slot are considered as lost.

D. Definition of EC

a) Loss-probability-aware ECs: With RSA, the utilization factor ρ_l of the lth CC is defined as,

$$\rho_l \triangleq \frac{\sum_{k=1}^{K} M_{lk} p_k B_k^u}{(1-\theta) B_l^{cc}}, \qquad (3)$$

where M_{lk} is the number of admitted class-k users in lth CC, and B_k^u is the effective bandwidth provided by the operator for each class-k user. When ρ_l equals to 1, the spectrum utilization can be maximized, however, the loss probabilities for some class k may exceed δ_k. Thus to keep the loss probability of each class under the desired level, ρ_l should be less than 1. To this end, the loss-probability-aware EC for class k in lth CC, denoted as N_{lk}, is defined as the maximum M_{lk} that satisfies the loss probability requirement δ_k, given specified bandwidth allocation strategy and bandwidth weights $\{\omega_{lk}\}$ (or $\{\omega_{lk}^{\max}\}$). With the derived EC set $\{N_{lk}\}$, a class-k user will be admitted if the current number of admitted class-k users is less than N_{lk}. As different ω_{lk} (or $\omega_{lk}^{\max}$) can result in different ECs, the tradeoff among the bandwidth weights is further discussed in Section VI for both bandwidth allocation strategies.

b) Mapping from minimum required throughput to the effective bandwidth: As EC is defined on a bandwidth basis, the user's minimum throughput requirement should be mapped into bandwidth requirement to be included in (3). As aforementioned in Section I, in a wireless mobile environment, the time-varying channel conditions make it difficult for the operators to provide a unified bandwidth to satisfy the minimum throughput requirement r_k^u for all the class-k users at one time. To this end, effective bandwidth is exploited to derive a unified bandwidth B_k^u to provide probabilistic QoS guarantee for all class-k users. In particular, the bandwidth B_k^u should be chosen such that

$$\sup_t \Pr\left\{ B_k^{u,ins}(t) \geq B_k^u \right\} \leq e(0 < e \ll 1), \qquad (4)$$

is satisfied, where $B_k^{u,ins}(t)$ denotes the instantaneous minimum required bandwidth to guarantee r_k^u at time t, and e is the upper bound of the QoS violation probability. Equation (4) indicates that given the statistical behaviors of the co-channel interference, the constant bandwidth B_k^u provided by the operator to each class-k user should be no less than $B_k^{u,ins}(t)$ with probability $1 - e$. In this way, the effective bandwidth B_k^u provides a bridge between the throughput requirement r_k^u and the EC N_{lk} over the wireless channel statistics. In this paper, we mainly focus on the intra-band CA [30], where all the CCs are located in the same frequency band and thus have the same radio channel statistics.

IV. EQUIVALENT CAPACITIES WITH FIXED BANDWIDTH ALLOCATION WEIGHTS

The fixed-weight bandwidth allocation strategy is analyzed in this section. Specifically, we first show how to obtain the user effective bandwidth from the throughput requirement, considering the multi-cell co-channel interference. Then, the analysis on a single CC is conducted to find the closed-form $\{N_{lk}\} - B_l^{cc}$ relationship, subject to the user equivalent QoS requirements (i.e., B_k^u and δ_k) and traffic descriptors (i.e., active probability p_k). The results are further extended to an LTE-A system with n aggregated CCs, where the ECs are compared between LTE and LTE-A users under the same system setting.

A. Effective Bandwidth From User Throughput Requirement

For downlink LTE-A systems, as users within the same cell are assigned with orthogonal PRBs, there is no interference among themselves. The co-channel interference is only from other cells that use the same PRBs with the considered cell. According to the LTE-A standard [10], the frequency reuse factor of LTE-A systems is 1, which means each cell operates on the same spectrum and the co-channel interference of the considered cell is the summation of the interference from all the other cells in area A. For a probabilistic analysis, the statistical behaviors of the user SINR (i.e., user SINR distributions) are required. Our previous work [33] has applied the Stochastic geometry [34] to provide tractable probabilistic interference modeling for users in LTE-A systems. Therefore, based on [33], the detailed analysis for user SINR distribution and effective bandwidth is shown as follows.

The channel gain of a user consists of two parts: the path loss and fast fading. The shadowing effect is not considered since the shadowing is shown to be well approximated by the randomness of the Poisson distributed BS locations [35]. This is a strong justification that we can model the locations of BSs into a PPP. Denote the power spectral density (PSD) of the BS transmission power and noise power as P_t and N_0, respectively. Then, the PSD of the received power of a user from BS B is calculated as

$$P_r = P_t H D_B^{-\alpha}, \ B \in \Phi_{BS}, \qquad (5)$$

where H is the fast fading channel gain; D_B is the distance between the considered user to BS B; and α is the path loss exponent. Then the user SINR is calculated as

$$SINR_k = \frac{P_t H D_{B_0}^{-\alpha}}{\sum_{B \in \Phi_{BS}^{inf} \setminus B_0} P_t H^{inf} D_B^{-\alpha} + n_0}, \qquad (6)$$

where Φ_{BS}^{inf} denotes the set of interfering BSs in Φ_{BS} that transmit on the same bandwidth with the considered user; $\Phi_{BS}^{inf} \setminus B_0$ means the set of interfering BSs excluding B_0; and H^{inf} denotes the fast fading channel gain between the considered user and the interfering BSs. In this paper, the fast fading between the considered user and the serving BS B_0 is Rayleigh fading, and the fast fading between the considered user and the interfering BSs is generally distributed. Therefore, the probability density function of H is an exponential distribution with parameter μ. For simplicity, μ is set to 1.

To obtain the SINR distribution for one user, we calculate the cumulative probability function (cdf) of $SINR_k$. The probability that $SINR_k$ is larger than a threshold T_k is

$$\mathbf{P}\{SINR_k > T_k\}$$

$$= \mathbf{P}\left\{\frac{P_t H D_{B_0}^{-\alpha}}{I + n_0} > T_k\right\} = \mathbf{P}\left\{H > \frac{(I + n_0)D_{B_0}^{\alpha} T_k}{P_t}\right\}$$

where $I = \sum_{B \in \Phi_{BS}^{inf} \backslash B_0} P_t H^{inf} D_B^{-\alpha}.$ (7)

Following the procedure in [33], the final result of $\mathrm{P}(SINR_k > T_k)$ is given directly as

$$\mathbf{P}\{SINR_k \geq T_k\} = 1 - \int_0^{+\infty} 2\pi\lambda_{BS} r e^{-\pi\lambda_{BS} r^2} e^{-n_0 r^\alpha \frac{T_k}{P_t}}$$

$$\cdot \exp\left\{-2\pi\theta^{usa}\lambda_{BS}\rho(r, H^{inf}, T_k)\right\} dr,$$

where $\rho(r, H^{inf}, T_k) = -\frac{1}{2}r^2 + \frac{1}{2}r^2 E_{H^{inf}}\left\{e^{-T_k H^{inf}}\right.$

$$\left. + (T_k H^{inf})^{2/\alpha}\left[\Gamma\left(1 - \frac{2}{\alpha}, 0\right) - \Gamma\left(1 - \frac{2}{\alpha}, T_k H^{inf}\right)\right]\right\},$$

and $\Gamma(s, t) = \int_t^{+\infty} x^{s-1} e^{-x} dx.$ (8)

In (8), θ^{usa} is the bandwidth usage probability that one BS transmits on the same bandwidth with the considered user. If the worst case is considered, i.e., every BS transmits on the same bandwidth with the considered user, the bandwidth usage probability is equal to 1. According to (4), the effective bandwidth B_k^u should be chosen such that

$$\sup_t \mathbf{P}\left\{B_k^{u,ins}(t) \geq B_k^u\right\} \leq e(0 < e \ll 1),$$ (9)

that is,

$$\sup_t \mathbf{P}\left\{r_k^{u,ins}(t) \leq r_k^u\right\} \leq e(0 < e \ll 1),$$ (10)

where $B_k^{u,ins}(t)$ is the instantaneous required bandwidth of class-k user, and $r_k^{u,ins}(t)$ is the instantaneous achieved throughput when bandwidth B_k^u is assigned. The left hand side of (10) can be rewritten as

$$\sup_t \mathbf{P}\left\{r_k^{u,ins}(t) \leq r_k^u\right\} = \mathbf{P}\left\{B_k^u \log(1 + SINR_k) \leq r_k^u\right\} \leq e$$

$$\Rightarrow \mathbf{P}\{SINR_k \geq 2^{\frac{r_k^u}{B_k^u}} - 1\} \geq 1 - e \quad (11)$$

Let $T_k = 2^{r_k^u/B_k^u} - 1$. Based on (8), B_k^u can be finalized as the minimum integral multiple of $N_l^{sc} B_l^{sc}$ that satisfies (11), where $N_l^{sc} B_l^{sc}$ is the bandwidth for one PRB, and the constraint of integral multiple is due to the fact that one PRB is the minimum bandwidth allocation unit in LTE-A systems.
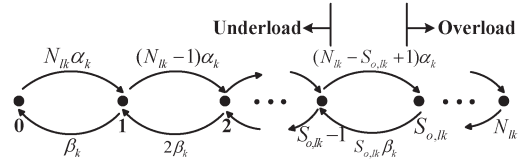

Fig. 4. Composite traffic model for the system states.

B. Equivalent Capacity for a Single Carrier

For the fixed-weight strategy, ω_{lk} is fixed, thus N_{lk} is only related to the parameters of class k. As aforementioned in Section III-D, if the utilization factor ρ_l equals to 1, the loss probability requirements may not be guaranteed. To control the loss probabilities below desired levels $\{\delta_k\}$, the bandwidth assigned to class k should be larger than the average bandwidth requirement of class k, i.e.,

$$B_{lk}^{cc} > N_{lk} p_k B_k^u, \ l = 1, 2, \ldots, n; \ k = 1, 2, \ldots, K, \quad (12)$$

where $B_{lk}^{cc} = \omega_{lk}(1 - \theta)B_l^{cc}$ is the bandwidth assigned to class-k users. ω_{lk} denotes the weight of B_{lk}^{cc}, satisfying $\sum_{k=1}^{K} \omega_{lk} = 1$. We intuitively and heuristically add some multiple of $\sigma_{lk} B_k^u$ to the right hand side of (12), where σ_{lk} is the standard deviation of the number of active class-k users in lth CC [36], thus satisfying $\sigma_{lk} = \sqrt{N_{lk} p_k(1 - p_k)}$, i.e.,

$$B_{lk}^{cc} = N_{lk} p_k B_k^u + \Gamma_k \sigma_{lk} B_k^u, \quad (13)$$

where Γ_k is a constant which varies with the specified QoS requirement (e.g., loss probability δ_k). Γ_k should increase when the QoS is more strictly defined (i.e., δ_k becomes smaller) while decrease approaching 0 when QoS is made more loose (i.e., δ_k becomes larger). In the following, systematic derivations are given to justify (13) with derived relation between Γ_k and δ_k. Substituting σ_{lk} into (13), we can get

$$B_{lk}^{cc} = \left(N_{lk} p_k + \Gamma_k \sqrt{N_{lk} p_k(1 - p_k)}\right) B_k^u. \quad (14)$$

By normalizing the bandwidth B_{lk}^{cc} with B_k^u, we can obtain

$$B_{lk}^{cc,nor} = N_{lk} p_k + \Gamma_k \sqrt{N_{lk} p_k(1 - p_k)}, \quad (15)$$

where $B_{lk}^{cc,nor} = B_{lk}^{cc}/B_k^u$ is the normalized bandwidth, and $\lfloor B_{lk}^{cc,nor} \rfloor$, i.e., the largest integer smaller than $B_{lk}^{cc,nor}$, indicates the maximum number of class-k users that can be served concurrently by bandwidth B_{lk}^{cc}. With RSA method, $B_{lk}^{cc,nor} < N_{lk}$ should hold when $p_k < 1$.

In our analysis, all the users are on or off independently. Therefore, the N_{lk} class-k users, each with the traffic model described in Section III-C, give rise to the composite traffic model in Fig. 4. This model is essentially an $(N_{lk} + 1)$-state birth-death process, where state i indicates there are i active class-k users in the system. Due to the independency among all the users, the state-transition rate α_k, β_k of the traffic model of each user can be directly added together to form the

inter-state transition rates as shown in (16), where $R_{i,j}$ denotes the transition rate from state i to state j.

$$\begin{cases} R_{i,i+1} = (N_{lk} - i)\alpha_k, & 0 \le i \le N_{lk} - 1, \\ R_{i,i-1} = i\beta_k, & 1 \le i \le N_{lk}, \\ R_{i,j} = 0, & |i - j| \ne 1. \end{cases} \quad (16)$$

The overload state $S_{o,lk}$ is defined for each class k as $S_{o,lk} = \lceil B_{lk}^{cc,nor} \rceil$, which is the minimum integer larger than $B_{lk}^{cc,nor}$. The state $S_{o,lk}$ is the critical state above which loss will occur, i.e, the system is overloaded. We now calculate the steady-state probabilities $\{\pi_{ik}\}(i = 1, \dots, N_{lk})$ that the system is in state i. As all the users are independent, the probabilities $\{\pi_{ik}\}$ follow the binomial distribution, where i out of N_{lk} users are active and the other $(N_{lk} - i)$ are off. Therefore, we have

$$\pi_{ik} = C_{N_{lk}}^i p_k{}^i (1 - p_k)^{N_{lk}-i}, \quad i = 0, 1, \dots, N_{lk}, \quad (17)$$

where $C_{N_{lk}}^i$ is the number of choices when picking i out of N_{lk}. With $\{\pi_i\}$, the loss probability δ_k can be calculated as the summation of π_{ik} of all the overload states, i.e.,

$$\delta_k = \sum_{i=S_{o,lk}}^{N_{lk}} \pi_{ik}. \quad (18)$$

It is well known that when $N_{lk} \gg 1$ and p_k is much smaller than 1, the binomial distribution π_{ik} can be closely approximated by the normal distribution with the mean value $N_{lk}p_k$ and variance $\sigma_{lk}^2 = N_{lk}p_k(1 - p_k)$ [37]. In this paper, this condition is satisfied for large number of class-k users with bursty traffic. We convert i and summation to continuous variable x and integrals, respectively, and then the loss probability δ_k is approximated by

$$\delta_k \approx \int_{S_{o,lk}}^{+\infty} \frac{e^{-(x-N_{lk}p_k)^2/(2\sigma_{lk}^2)}}{\sqrt{2\pi}\sigma_{lk}} dx = \int_{\frac{S_{o,lk}-N_{lk}p_k}{\sqrt{2}\sigma_{lk}}}^{+\infty} \frac{e^{-y^2}}{\sqrt{\pi}} dy, \quad (19)$$

where the second step is achieved by replacing x with $\sqrt{2}\sigma_{lk}y + N_{lk}p_k$. Then, integration by parts method is applied to keep the dominant parts of the integration. By multiplying numerator and denominator of the integral by y, we have,

$$\int_z^{+\infty} \frac{ye^{-y^2}}{y} dy = \frac{e^{-z^2}}{2z} - \frac{e^{-z^2}}{4z^3} + \frac{3}{4}\int_z^{+\infty} \frac{e^{-y^2}}{y^4} dy, \quad (20)$$

where $z = (S_{o,lk} - N_{lk}p_k)/\sqrt{2}\sigma_{lk}$. When z is greater than 3 (can be easily guaranteed in our setting), the first two items on the RHS of (20) are much larger than the third one. Therefore, we can obtain

$$\int_z^{+\infty} e^{-y^2} dy \approx \left(\frac{e^{-z^2}}{2z} - \frac{e^{-z^2}}{4z^3} \right). \quad (21)$$

Finally, since $S_{o,lk} \approx B_{lk}^{cc,nor}$, combining (19)–(21), we derive the expression of loss probability δ_k as,

$$\delta_k \approx \frac{\sigma_{lk} e^{-\left(B_{lk}^{cc,nor} - N_{lk}p_k\right)/2\sigma_{lk}{}^2}}{\sqrt{2\pi}\left(B_{lk}^{cc,nor} - N_{lk}p_k\right)}. \quad (22)$$

Take natural logs for both sides of (22), we have

$$\ln(\sqrt{2\pi}\delta_k) = \ln \frac{\sigma_{lk}}{(B_{lk}^{cc,nor} - N_{lk}p_k)} - \frac{(B_{lk}^{cc,nor} - N_{lk}p_k)^2}{2\sigma_{lk}{}^2}. \quad (23)$$

The first item on the RHS of (23) is neglectable compared with the second, so (23) can be further simplified and rearranged as

$$B_{lk}^{cc,nor} \approx N_{lk}p_k + \sigma_{lk}\sqrt{-2\ln\delta_k - \ln(2\pi)}. \quad (24)$$

Now, the previously proposed heuristic thought in (15) is justified with $\Gamma_k = \sqrt{-2\ln\delta_k - \ln(2\pi)}$, and N_{lk} can be solved easily from (24),

$$N_{lk} = \left\lfloor \frac{B_{lk}^{cc,nor}}{p_k} - \frac{1}{p_k}\left[\sqrt{4\lambda_k\left(B_{lk}^{cc,nor} + \lambda_k\right)} - 2\lambda_k\right]\right\rfloor,$$

where

$$\lambda_k = \Gamma_k^2(1 - p_k)/4, \; B_{lk}^{cc,nor} = \omega_{lk}(1-\theta)B_l^{cc}/B_k^u. \quad (25)$$

Therefore, combining (12), (15), and (25), we can finally conclude that for the lth CC, given fixed bandwidth weight ω_{lk}, users' effective bandwidth B_k^u, loss probability δ_k, active probability p_k, the normalized bandwidth $B_{lk}^{cc,nor}$ and the EC N_{lk} have the relationship shown in (25) for each class k.

C. EC Comparison in Multi-Carrier LTE-A Systems

The ECs between LTE users and LTE-A users for each class k are compared in this subsection. n CCs are considered. For the LTE users, as they cannot aggregate PRBs from different CCs, the total EC for class k, denoted as N_k^{LTE}, should be the summation of every N_{lk}. Hence we have,

$$N_k^{LTE} = \sum_{l=1}^n N_{lk}$$

$$= \sum_{l=1}^n \left\lfloor \frac{B_{lk}^{cc,nor}}{p_k} - \frac{1}{p_k}\left[\sqrt{4\lambda_k\left(B_{lk}^{cc,nor} + \lambda_k\right)} - 2\lambda_k\right]\right\rfloor,$$

where

$$\lambda_k = \Gamma_k^2(1-p_k)/4, \Gamma_k = \sqrt{-2\ln\delta_k - \ln(2\pi)},$$

$$B_{lk}^{cc,nor} = \omega_{lk}(1-\theta)B_l^{cc}/B_k^u. \quad (26)$$

For LTE-A users, they can use PRBs from different CCs to transmit concurrently on a wider aggregated virtual bandwidth. The normalized virtual bandwidth for each class k is

$\sum_{l=1}^{n} B_{lk}^{cc,nor}$. Therefore, the total EC for class k, denoted as N_k^{LTE-A}, is given below,

$$N_k^{LTE-A}$$
$$= \begin{cases} N_k^{LTE}, & \text{if } \left\lfloor \sum_{l=1}^{n} B_{lk}^{cc,nor} \right\rfloor - \sum_{l=1}^{n} \left\lfloor B_{lk}^{cc,nor} \right\rfloor < 1; \\ \left\lfloor \dfrac{\sum_{l=1}^{n} B_{lk}^{cc,nor}}{p_k} - \dfrac{1}{p_k} \left[\sqrt{4\lambda_k \left(\sum_{l=1}^{n} B_{lk}^{cc,nor} + \lambda_k \right)} - 2\lambda_k \right] \right\rfloor, \\ \text{otherwise}, \end{cases}$$
$$\tag{27}$$

with the same λ_k, Γ_k, and B_{lk} defined in (26). From (26) and (27), we can observe that the ECs of both LTE and LTE-A users increase when one of the following situations occurs: *i)* the active probability p_k decreases, *ii)* the maximum loss probability δ_k increases, or *iii)* the normalized bandwidth $B^{cc,nor}$ increases. Besides, when $\lfloor \sum_{l=1}^{n} B_{lk}^{cc,nor} \rfloor - \sum_{l=1}^{n} \lfloor B_{lk}^{cc,nor} \rfloor < 1$, the maximal number of LTE-A users that can be concurrently served is equal to that of LTE users, since even combining the left PRBs of all CCs is not enough to support one more user. In this situation, N_k^{LTE-A} and N_k^{LTE} are equal, which is called the zero-gain situation. However, when it is not the case, more PRBs will be used by LTE-A users for multi-CC transmission, and N_k^{LTE-A} will be larger than N_k^{LTE}, which will be verifed in Section VII.

V. EQUIVALENT CAPACITIES WITH COGNITIVE BANDWIDTH ALLOCATION WEIGHTS

In this section, the cognitive-weight strategy is studied. Similar to Section IV, we first derive the closed-from expression in single-carrier LTE-A systems and then extend the expression to multi-carrier case where the ECs between LTE and LTE-A users are compared. For the sake of analytical simplicity and presentation, we only show the closed-form results and conduct simulations for the two-user-class case. The methodology to obtain the results for generalized cases is also given in the last.

A. Single-Carrier Case

In this section, we consider downlink transmission in a single carrier with only two user classes. Without loss of generality, class 1 is assumed with higher priority than class 2. We follow the effective bandwidth mapping procedure in Section IV. All the previous notations are applicable in this section. Moreover, we denote $\omega_{l1}^{\max}$ as the maximal bandwidth weight for class 1 in lth CC, thus $\omega_{l1} \leq \omega_{l1}^{\max}$. Then, the maximal number of class-1 users that can be served concurrently by lth CC (denoted as K_{l1}) is

$$K_{l1} = \left\lfloor \frac{B_l^{cc} \omega_{l1}^{\max}(1-\theta)}{B_1^u} \right\rfloor. \tag{28}$$

Given the number of class-1 users concurrently being served, i.e., n_{l1}, the maximum number of class-2 users that can be concurrently served by lth CC, denoted as $K_{l2}(n_{l1})$, can be expressed as

$$K_{l2}(n_{l1}) = \begin{cases} \lfloor a(n_{l1}) \rfloor, & \text{if } n_{l1} \leq K_{l1}; \\ \lfloor a(K_{l1}) \rfloor, & \text{if } n_{l1} > K_{l1}; \end{cases} \tag{29}$$

where $a(\cdot)$ is a function defined as

$$a(x) \triangleq \frac{B_l^{cc}(1-\theta) - xB_1^u}{B_2^u}. \tag{30}$$

As aforementioned, all the users are on or off independently with the traffic generation model described in Section III-C. Thus the N_{l1} class-1 and N_{l2} class-2 users can form two independent birth-death processes with $(N_{l1} + 1)$ and $(N_{l2} + 1)$ states, respectively, as shown in Fig. 4. Having preemptive priority over class-2 users, a class-1 user can get served immediately as long as $\omega_{l1} \leq \omega_{l1}^{\max}$ after it is accepted. As a result, the overload state of class 1 is fixed while that of class 2 changes with n_{l1},

$$S_{o,l1} = K_{l1} + 1, \quad S_{o,l2} = K_{l2}(n_{l1}) + 1. \tag{31}$$

Given the loss probability requirement δ_1 and active probability p_1 of class-1 users, the EC N_{l1} can be calculated similarly as (25),

$$N_{l1} = \left\lfloor \frac{K_{l1}}{p_1} - \frac{1}{p_1} \left[\sqrt{4\lambda_1(K_{l1} + \lambda_1)} - 2\lambda_1 \right] \right\rfloor,$$

$$\text{where} \quad \lambda_1 = \frac{\Gamma_1^2(1-p_1)}{4}, \ \Gamma_1 = \sqrt{-2\ln\delta_1 - \ln(2\pi)}. \tag{32}$$

The calculation of N_{l2} is the most challenging part of the derivation. Different from the fixed-weight strategy, N_{l2} in the cognitive-weight strategy is closely related to the current number of admitted class-1 users (denoted as N_{l1}^{ad}). N_{l1}^{ad} is considered to be $K_{l1} \ll N_{l1}^{ad} \leq N_{l1}$, because the number of admitted users can be much larger than the maximum number of users that can be concurrently served due to the small active probability p_1 in the considered scenarios.

Given N_{l1}^{ad}, $\omega_{l1}^{\max}$ and loss probability requirement δ_2, we still exploit the binomial-normal approximation to get a closed-form relationship between B_l^{cc} and N_{l2}. With the steady-state probabilities $\{\pi_{i1}\}$ and $\{\pi_{i2}\}$, the loss probability of class-2 users can be calculated with two parts,

$$\delta_2 = \underbrace{\sum_{n_{l1}=0}^{K_{l1}} \pi_{n_{l1}1} \sum_{n_{l2}=\lfloor a(n_{l1}) \rfloor+1}^{N_{l2}} \pi_{n_{l2}2}}_{A_1}$$

$$+ \underbrace{\sum_{n_{l1}=K_{l1}+1}^{N_{l1}^{ad}} \pi_{n_{l1}1} \sum_{n_{l2}=\lfloor a(K_{l1}) \rfloor+1}^{N_{l2}} \pi_{n_{l2}2}}_{A_2}.$$

$$\text{where} \quad pi_{n_{l1}1} = C_{N_{l1}^{ad}}^{n_{l1}} p_1^{n_{l1}} (1-p_1)^{N_{l1}^{ad}-n_{l1}},$$

$$\pi_{n_{l2}2} = C_{N_{l2}}^{n_{l2}} p_2^{n_{l2}} (1-p_2)^{N_{l2}-n_{l2}},$$

$$n_{l1} = 0, 1, \ldots, N_{l1}^{ad}, n_{l2} = 0, 1, \ldots, N_{l2}. \tag{33}$$

A_1 is the loss probability of class-2 users when there is no loss from class-1. A_2 is the loss probability when the loss of

class 1 occurs, i.e., maximal bandwidth allocation weight $\omega_{l1}^{\max}$ is reached. Similar as Section IV, since $N_{l1}^{ad} \gg 1$, $N_{l2} \gg 1$, and $p_k \ll 1 (k = 1, 2)$, the steady-state probabilities $\{\pi_{n_{lk}k}\}$ can be approximated by normal distribution with mean value $N_{l1}^{ad} p_1$ (or $N_{l2} p_2$) and variance $\sigma_{l1}^2 = N_{l1}^{ad} p_1(1 - p_1)$ (or $\sigma_{l2}^2 = N_{l2} p_2(1 - p_2)$) as shown below,

$$\delta_2 = \int\limits_{-\infty}^{K_{l1}} \frac{e^{-\left(x - N_{l1}^{ad} p_1\right)^2 / \left(2\sigma_{l1}^2\right)}}{\sqrt{2\pi}\sigma_{l1}} \int\limits_{a(x)}^{+\infty} \frac{e^{-(y - N_{l2} p_2)^2 / \left(2\sigma_{l2}^2\right)}}{\sqrt{2\pi}\sigma_{l2}} \, dy \, dx$$

$$+ \int\limits_{K_{l1}}^{+\infty} \frac{e^{-\left(x - N_{l1}^{ad} p_1\right)^2 / \left(2\sigma_{l1}^2\right)}}{\sqrt{2\pi}\sigma_{l1}} \int\limits_{a(K_{l1})}^{+\infty} \frac{e^{-(y - N_{l2} p_2)^2 / \left(2\sigma_{l2}^2\right)}}{\sqrt{2\pi}\sigma_{l2}} \, dy \, dx.$$

$$(34)$$

We first calculate A_1. Similar as (19)–(21), we utilize integration by parts to keep the dominant parts of the single integral with respect to variable y. Then the double integral A_1 is turned into single integral with respect to x as

$$A_1 \approx \underbrace{\frac{1}{\sqrt{2\pi}\sigma_{l1}} \int\limits_{-\infty}^{K_{l1}} \frac{e^{-\frac{\left(x - N_{l1}^{ad} p_1\right)^2}{2\sigma_{l1}^2} - \frac{[a(x) - N_{l2} p_2]^2}{2\sigma_{l2}^2}}}{\sqrt{2}\left[a(x) - N_{l2} p_2\right]/\sigma_{l2}} \, dx}_{A_3}$$

$$- \underbrace{\frac{1}{\sqrt{2\pi}\sigma_{l1}} \int\limits_{-\infty}^{K_{l1}} \frac{e^{-\frac{\left(x - N_{l1}^{ad} p_1\right)^2}{2\sigma_{l1}^2} - \frac{[a(x) - N_{l2} p_2]^2}{2\sigma_{l2}^2}}}{\sqrt{2}\left[a(x) - N_{l2} p_2\right]^3/\sigma_{l2}^3} \, dx}_{A_4}. \quad (35)$$

The approximation holds when $[a(x) - N_{l2} p_2]/(\sqrt{2}\sigma_2) > 3$ for all $x \in (-\infty, K_{l1})$, which can be easily satisfied by our settings. We continue to calculate A_3 as labelled in (35). Redefine $z = a(x) - N_{l2} p_2$ and A_3 can be rewritten as

$$A_3 = \frac{\sigma_{l2} B_2^u}{\sqrt{2} B_1^u} \int\limits_{a(K_{l1}) - N_{l2} p_2}^{+\infty} e^{-\frac{\left[r - N_{l1} p_1 - \left(B_2^u/B_1^u\right)z\right]^2}{2\sigma_{l1}^2} - \frac{z^2}{2\sigma_{l2}^2}} \frac{dz}{z}$$

$$= \frac{\sigma_{l2} B_2^u}{\sqrt{2} B_1^u} \int\limits_{a(K_{l1}) - N_{l2} p_2}^{+\infty} \frac{e^{-C_1 z^2} - C_2 z + C_3}{z} \, dz,$$

where

$$C_1 = \frac{\left(\frac{B_2^u}{B_1^u}\right)^2}{2\sigma_{l1}^2} + \frac{1}{2\sigma_{l2}^2} > 0, \quad C_2 = \frac{B_2^u \left(N_{l1}^{ad} p_1 - r\right)}{\sigma_{l1}^2 B_1^u},$$

$$C_3 = -\frac{\left(N_{l1}^{ad} p_1 - r\right)^2}{2\sigma_{l1}^2},$$

$$r = \frac{B_2^u + B_l^{cc}(1 - \theta) - N_{l2} p_2 B_2^u}{B_1^u}$$

$$\approx \frac{B_l^{cc}(1 - \theta) - N_{l2} p_2 B_2^u}{B_1^u}. \quad (36)$$

As C_1 is positive, we can still use integration by parts to only keep the dominant first two items,

$$A_3 \approx \frac{\sigma_{l2} B_2^u}{\sqrt{2} B_1^u} \left[\frac{1}{2C_1 \eta^2 + C_2 \eta} - \frac{4C_1 \eta + C_2}{(2C_1 \eta + C_2)(2C_1 \eta^2 + C_2 \eta)^2} \right]$$

$$\cdot e^{-C_1 \eta^2 - C_2 \eta + C_3},$$

$$\text{where} \quad \eta = a(K_{l1}) - N_{l2} p_2. \quad (37)$$

A_4 can be approximated in the same way and given as

$$A_4 \approx \frac{\sigma_{l2}^3 B_2^u}{\sqrt{2} B_1^u} \left[\frac{1}{\eta^3(2C_1 \eta + C_2)} - \frac{8C_1 \eta^3 + 3C_2 \eta^2}{(2C_1 \eta^4 + C_2 \eta^2)^2 (2C_1 \eta + C_2)} \right]$$

$$\cdot e^{-C_1 \eta^2 - C_2 \eta + C_3}. \quad (38)$$

Now we have derived the first part A_1 of loss probability δ_2 with the summation of A_3 and A_4 as shown in (37) and (38). The second part A_2 is easier to calculate, since the two integrals in A_2 are independent with each other and thus can be viewed as the product of two single integrals with respect to x and y, respectively. Applying the integration by parts method, we can get the value of A_2 as

$$A_2 \approx \frac{1}{\pi} \frac{\left(2z_1^2 - 1\right)}{4z_1^3} \frac{\left(2z_2^2 - 1\right)}{4z_2^3} e^{-C_1 \eta^2 - C_2 \eta + C_3},$$

$$\text{where} \quad z_1 = \frac{\left(K_{l1} - N_{l1}^{ad} p_1\right)}{\left(\sqrt{2}\sigma_{l1}\right)},$$

$$z_2 = \frac{[a(K_{l1}) - N_{l2} p_2]}{\left(\sqrt{2}\sigma_{l2}\right)}. \quad (39)$$

Equations (37)–(39) can hold only if both z_1 and z_2 are larger than 3, which can be satisfied by our settings. It can be seen that A_3, A_4 and A_2 all have the same exponential part $e^{-C_1 \eta^2 - C_2 \eta + C_3}$. Let ζ denote the summation of all the coefficients of the exponentials from A_1 and A_2. By taking natural logs for the loss probability δ_2, we can have

$$\ln(\delta_2) = \ln(\zeta) - C_1 \eta^2 - C_2 \eta + C_3, \; \zeta > 0. \quad (40)$$

The first item of RHS in (40) is neglectable compared with the remaining items, thus (40) can be further simplified as

$$\ln(\delta_2) \approx -C_1 \eta^2 - C_2 \eta + C_3, \quad (41)$$

Finally, by solving N_{l2} from (41), the closed-form relationship between EC N_{l2} and the system bandwidth B_l^{cc} can be obtained given N_{l1}^{ad}, δ_2, p_2 and $\omega_{l1}^{\max}$,

$$N_{l2} = \left\lfloor \frac{a(K_{l1})}{p_2} - \frac{1}{p_2} \left[\sqrt{4\lambda_{2l} \left(a(K_{l1}) + \lambda_{2l}\right)} - 2\lambda_{2l} \right] \right\rfloor,$$

$$\text{where} \quad \lambda_{2l} = \frac{\Gamma_{2l}^2 (1 - p_2)}{4},$$

$$\Gamma_{2l} = \sqrt{-2\ln(\delta_2) - \left(K_{l1} - N_{l1}^{ad} p_1\right)^2 / \sigma_{l1}^2}. \quad (42)$$

From (42), we can observe that the structure of the closed-form relationship of EC N_{l2} is very similar to that of N_{l1} (i.e., (32)), except that i) $a(K_{l1})$ is the maximal number of class-2 users that can be concurrently served by lth CC when ω_{l1} reaches its maximum, and ii) Γ_{2l} is not only related to loss probability δ_2 but also modulated by the parameters of class 1. Furthermore, with the decrease of δ_2 or the increase of $\omega_{l1}^{\max}$, λ_{2l} will increase and EC N_{l2} will decrease accordingly, which satisfies the intuitions.

B. Multi-Carrier Case: LTE Users vs. LTE-A Users

In this subsection, we extend the derived closed-form expression of EC under the cognitive-weight strategy to the multi-carrier case with n aggregated CCs. Similar as Section IV-C, the ECs become different between LTE users and LTE-A users. For the LTE users, as they cannot use PRBs from different CCs concurrently, the total EC for class $k(k = 1, 2)$, denoted as N_k^{LTE}, should be the summation of every N_{lk}, as shown below,

$$N_1^{LTE} = \sum_{l=1}^{n} N_{l1}$$

$$= \sum_{l=1}^{n} \left\lfloor \frac{K_{l1}}{p_1} - \frac{1}{p_1} \left[\sqrt{4\lambda_1(K_{l1} + \lambda_1)} - 2\lambda_1 \right] \right\rfloor,$$

$$N_2^{LTE} = \sum_{l=1}^{n} N_{l2}$$

$$= \sum_{l=1}^{n} \left\lfloor \frac{a(K_{l1})}{p_2} - \frac{1}{p_2} \left[\sqrt{4\lambda_{2l}(a(K_{l1}) + \lambda_{2l})} - 2\lambda_{2l} \right] \right\rfloor,$$

where

$$\lambda_1 = \frac{\Gamma_1^2(1 - p_1)}{4}, \ \Gamma_1 = \sqrt{-2\ln(\delta_1) - \ln(2\pi)},$$

$$\lambda_{2l} = \frac{\Gamma_{2l}^2(1 - p_2)}{4},$$

$$\Gamma_{2l} = \sqrt{-2\ln(\delta_2) - (K_{l1} - N_{l1}^{ad}p_1)^2 / \sigma_{l1}^2},$$

$$K_{l1} = \left\lfloor \frac{B_l^{cc}\omega_{l1}^{\max}(1 - \theta)}{B_1^u} \right\rfloor. \tag{43}$$

On the other hand, LTE-A users can use PRBs from different CCs to transmit concurrently on a wider aggregated virtual bandwidth. For class 1 with higher priority, the aggregated virtual bandwidth is $\sum_{l=1}^{n} B_l^{cc}(1 - \theta)\omega_{l1}^{\max}$. Define

$$K_1 := \left\lfloor \frac{\sum_{l=1}^{n} B_l^{cc}(1 - \theta)\omega_{l1}^{\max}}{B_1^u} \right\rfloor,$$

$$\hat{a}(x) := \frac{[\sum_{l=1}^{n} B_l^{cc}(1 - \theta) - xB_1^u]}{B_2^u}. \tag{44}$$

Then the maximal number of class-2 users that can be concurrently served by n CCs is $\hat{a}(K_1)$ when $\sum_{l=1}^{n} \omega_{l1}$ reaches the maximum. Thus the total EC of class $k(k = 1, 2)$, denoted as N_k^{LTE-A}, is given as,

$$N_1^{LTE-A}$$

$$= \begin{cases} N_1^{LTE}, \text{ if } K_1 - \sum_{l=1}^{n} K_{l1} < 1; \\ \left\lfloor \frac{K_1}{p_1} - \frac{1}{p_1} \left[\sqrt{4\lambda_1(K_1 + \lambda_1)} - 2\lambda_1 \right] \right\rfloor, \text{ otherwise;} \end{cases}$$

$$N_2^{LTE-A}$$

$$= \begin{cases} N_2^{LTE}, \text{ if } K_1 - \sum_{l=1}^{n} K_{l1} < 1 \ and \\ \hat{a}\left(\sum_{l=1}^{n} n_{l1}\right) - \sum_{l=1}^{n} K_{l2}(n_{l1}) < 1, \ \forall n_{l1} \le K_{l1}; \\ \left\lfloor \frac{\hat{a}(K_1)}{p_2} - \frac{1}{p_2} \left[\sqrt{4\lambda_2(\hat{a}(K_1) + \lambda_2)} - 2\lambda_2 \right] \right\rfloor, \text{ otherwise} \end{cases}$$

where

$$\lambda_1 = \frac{\Gamma_1^2(1 - p_1)}{4}, \ \Gamma_1 = \sqrt{-2\ln(\delta_1) - \ln(2\pi)},$$

$$\lambda_2 = \frac{\Gamma_2^2(1 - p_2)}{4},$$

$$\Gamma_2 = \sqrt{-2\ln(\delta_2) - \left(K_1 - \sum_{l=1}^{n} N_{l1}^{ad}p_1\right)^2 / \sigma_1^2},$$

$$\sigma_1^2 = \sum_{l=1}^{n} N_{l1}^{ad}p_1(1 - p_1). \tag{45}$$

Under this strategy, the zero-gain situation will hardly occur since its occurrence conditions are much harder due to that the bandwidth weight of class-2 users can dynamically change in a cognitive manner as the secondary users do in the cognitive radio networks.

C. Generalization of the Loss Probability Derivation

This subsection gives the generalized derivation of the loss probability δ_k given K user classes in the lth CC. Without loss of generality, we consider descending priorities from class 1 to class K. The maximum bandwidth weights of class k is $\omega_{lk}^{\max}$, and $\omega_{l1}^{\max} < \cdots < \omega_{lk}^{\max} < \cdots < \omega_{lK}^{\max} = 1$. As $\delta_k(k > 1)$ is related to the parameters of user classes with higher priorities, it can be expressed as a function of $\omega_{lm}^{\max}(m = 1, \ldots, k)$ and the current numbers of admitted users of the first $k - 1$ classes (i.e., $N_{lm}^{ad}, m = 1, \ldots, k - 1$) in the following

$$\delta_k = \sum_{x_m \in \{0,1\}, m=1 \sim k-1} p_{x_1 \ldots x_{k-1}}\left(\omega_{l1}, \ldots, \omega_{lk}, N_{l1}^{ad}, \ldots, N_{l(k-1)}^{ad}\right)$$

$$\tag{46}$$

where x_m is a binary variable taking 0 when there is no loss from class m and 1 otherwise. The $p_{x_1 \ldots x_{k-1}}(\cdot)$ is the loss probability of class k given the values of $x_1, \ldots, x_{k-1}$, which can be further calculated as,

$$p_{x_1 \ldots x_{k-1}}\left(\omega_{l1}, \ldots, \omega_{lk}, N_{l1}^{ad}, \ldots, N_{l(k-1)}^{ad}\right)$$

$$= \sum_{n_{l1}=\mu_1}^{\eta_1} \pi_{n_{l1}1} \cdots \sum_{n_{lm}=\mu_m}^{\eta_m} \pi_{n_{lm}m} \cdots \sum_{n_{lk}=\mu_k}^{N_{lk}} \pi_{n_{lk}k},$$

where

$$\mu_m = \begin{cases} 0, \text{ if } x_m = 0, \ 1 \le m < k; \\ \left\lfloor \frac{B_l^{cc}\omega_{l1}^{max}}{B_1^u} \right\rfloor + 1, \text{ if } x_1 = 1; \\ a_m(\omega_{l1}, \ldots, \omega_{lm}, x_1, \ldots, x_{m-1}) + 1, \\ \qquad \text{ if } x_m = 1, \ 1 < m < k; \end{cases}$$

$$\eta_m = \begin{cases} \left\lfloor \frac{B_l^{cc}\omega_{l1}^{max}}{B_1^u} \right\rfloor, \text{ if } x_1 = 0; \\ a_m(\omega_{l1}, \ldots, \omega_{lm}, x_1, \ldots, x_{m-1}), \\ \qquad \text{ if } x_m = 0, \ 1 < m < k; \\ N_{lm}^{ad}, \text{ if } x_m = 1, \ 1 \le m < k; \end{cases}$$

$$a_m(\omega_{l1}, \ldots, \omega_{lm}, x_1, \ldots, x_{m-1})$$

$$= \left\lfloor \frac{\left\lfloor B_l^{cc}(\omega_{lm}^{max} - \hat{\omega}_{lm^*}^{max}) - \sum\limits_{b=m^*+1}^{m-1} B_b^u \cdot n_{lb} \right\rfloor}{B_m^u} \right\rfloor;$$

$$m^* = \begin{cases} 0, \text{ if } \forall\, x_b = 0, \ 1 \le b < m. \\ \arg\max\limits_{1 \le b < m, \ x_b = 1} b, \text{ otherwise.} \end{cases} \tag{47}$$

The physical meaning of $a_m(\cdot)$ is the maximum number of class-m users that can be concurrently served by lth CC given ω_{lk}^{max}, x_k, and n_{lk} of all classes with priorities higher than m. With similar binomial-normal approximation approach, each summation in (47) can be turned into one integral. Therefore, to calculate the closed-form expression of δ_k, 2^{k-1} items will be summed together (see (46)), and each item is a k-fold integral (see (47)). However, with higher k, the approximation accuracy will be lower as the difference between the exact and approximated values accumulates with integrals.

VI. NET-PROFIT MAXIMIZATION UNDER DIFFERENT BANDWIDTH ALLOCATION STRATEGIES

In previous sections, we have derived the closed-form expressions of ECs considering user loss probability requirements for both LTE and LTE-A users under the fixed-weight and cognitive-weight strategies. In this section, we discuss the economic tradeoff among the bandwidth allocation weights of different user classes via a net-profit-maximization problem.

The decision of the bandwidth allocation weights depends on a combination of factors. Among these factors, operator profits, user satisfaction and the dynamic traffic conditions of different user classes are the three most important ones. On one hand, the operators tend to allocate more bandwidth to the user class that can bring higher profits per PRB, i.e., short-term profits. On the other hand, only maximizing the short-term profits may incur undesired user dissatisfaction for some kinds of user classes, which may in turn hurt the operators' long-term benefits. Therefore, the optimal decision of the bandwidth allocation weights should balance the operators' short-term profits and the satisfaction of all the user classes. Moreover, to enhance the bandwidth utilization, the weight decision should be conducted dynamically to adapt to the time-varying traffic conditions of different user classes.

To formulate the tradeoff into an optimization problem, we consider that the average number of users for each class k in a cell is constant within a certain time period τ but changes from period to period. For a particular τ, denote the average number of class-k users in the cell as $N_k(\tau)$. The $N_k(\tau)$ users can be on or off following the traffic model in Section III-C. The profit per PRB achieved by the operator from class-k users is denoted as $G_{k,PRB}$. Our objective is to maximize the net benefits that the operator can get considering the user satisfaction factor for each period τ.

A. Fixed-Weight Bandwidth Allocation Strategy

For the fixed-weight strategy, the optimization problem for LTE users is given as

$$\max_{\omega_{lk}} \quad \sum_{k=1}^{K} \left[\min\left\{N_k(\tau), N_k^{LTE}\right\} p_k \frac{B_k^u}{B_l^{sc} N_l^{sc}} G_{k,PRB} \right.$$
$$\left. - \chi_k \max\left\{N_k(\tau) - N_k^{LTE}, 0\right\} \right]$$

s.t. equation (26);
$$l = 1, 2, \ldots n; \quad k = 1, 2, \ldots, K, \tag{48}$$

where $\min\{N_k(\tau), N_k^{LTE}\}$ is the actual number of admitted class-k users and $\max\{N_k(\tau) - N_k^{LTE}, 0\}$ is the average number of class-k users that are rejected to get into the system. Thus $\min\{N_k(\tau), N_k^{LTE}\}p_k B_k^u/(B_l^{sc} N_l^{sc})$ is the average number of PRBs that are occupied by class-k users within period τ. χ_k is a weighting parameter to adjust the relative importance of class-k users' satisfaction over short-term profits. The optimization can be simplified by introducing auxiliary variables $\phi_k = \min\{N_k(\tau), N_k^{LTE}\}$ and $\varphi_k = \max\{N_k(\tau) - N_k^{LTE}, 0\}$,

$$\max_{\omega_{lk}} \quad \sum_{k=1}^{K} \left[\phi_k p_k \frac{B_k^u}{B_l^{sc} N_l^{sc}} G_{k,PRB} - \chi_k \varphi_k \right]$$

s.t. equation (18), $\quad \forall\, k = 1, 2, \ldots, K;$
$$\phi_k \le N_k(\tau), \quad \forall\, k = 1, 2, \ldots, K;$$
$$\phi_k \le N_k^{LTE}, \quad \forall\, k = 1, 2, \ldots, K;$$
$$\varphi_k \ge N_k(\tau) - N_k^{LTE}, \quad \forall\, k = 1, 2, \ldots, K;$$
$$\varphi_k \ge 0, \quad \forall\, k = 1, 2, \ldots, K;$$
$$0 \le \omega_{lk} \le 1. \tag{49}$$

The optimization problem (49) is a typical nonlinear programming problem which can be effectively solved following [38]. Similarly, for LTE-A users, the optimization problem is the same as (49) with replacing (26) with (27).

TABLE II
SIMULATION PARAMETERS I

Parameter Group 1	Values
Considered area, $|A|$	$20 \times 20 km^2$
Transmission power spectrum density, P_t	0.2 W/Hz
Noise power spectrum density, N_0	10^{-9} W/Hz
Path loss exponent, a	4
BS density, λ_{BS}	$1/(\pi 500^2) m^{-2}$
Fast fading of the interfering signals	Rayleigh fading
Subcarrier bandwidth, B_l^{sc}	15kHz
Number of subcarriers per PRB, N_l^{sc}	12

TABLE III
SIMULATION PARAMETERS II

Parameter Group 2	Class 1	Class 2
Number of CCs, n	$1\sim5$	$1\sim5$
CC bandwidth, B_l^{cc}	20MHz	20MHz
Number of PRBs per user, P_k^u	$8\sim20$	$1\sim10$
Loss probability, δ_k	$10^{-5}\sim10^{-1}$	$10^{-6}\sim10^{-3}$
Active probability, p_k	$0.02\sim0.2$	$0.02\sim0.2$
Total percentage of GBs, θ	0.1	0.1
Normalized profit, $G_{k,PRB}$	3	2
Satisfaction weighting factor, χ_k	0.075	0.05

B. Cognitive-Weight Bandwidth Allocation Strategy

For the cognitive-weight strategy, the optimization problem for LTE users is formulated similarly as

$$\max_{\omega_{l1}^{max}} \sum_{k=1}^{2} \Big[\min\{N_k(\tau), N_k^{LTE}\} p_k \frac{B_k^u}{B_l^{sc} N_l^{sc}} G_{k,PRB}$$

$$- \chi_k \max\{N_k(\tau) - N_k^{LTE}, 0\} \Big]$$

s.t. equation (43);

$$N_{l1}^{ad} = \frac{\min\{N_1(\tau), N_1^{LTE}\} \omega_{l1}^{max}}{\sum_{l=1}^{2} \omega_{l1}^{max}}. \tag{50}$$

The main difference of optimization problem (50) from (48) is the decision of N_2^{LTE}. In (50), N_2^{LTE} is closely related to the number of admitted class-1 users in each CC (i.e., N_{l1}^{ad}) and N_{l1}^{ad} is further limited by N_1^{LTE}; while in (48), N_2^{LTE} is only related to its own weight ω_{l2}, which is fixed for a certain τ. Therefore, the cognitive bandwidth allocation has stronger adaptability in capturing the time-varying traffic demands of different users, thus having higher bandwidth utilization. Here, we consider that all the admitted LTE users in the same class are assigned to different CCs in proportion to ω_{l1}^{max}. For LTE-A users, the optimization problem is the same as (50) except that i) (43) is replaced by (45); ii) the equation about N_{l1}^{ad} is replaced by $\sum_{l=1}^{n} N_{l1}^{ad} = \phi_1$ since all the CCs can be aggregated as a virtual band and it is not necessary to know the specific value of each N_{l1}^{ad}.

VII. SIMULATION RESULTS

To validate our proposed closed-form expressions of EC, system-level simulations are conducted for a multi-cell downlink scenario. Furthermore, the ECs are compared between LTE users and LTE-A users for both fixed-weight and cognitive-weight strategies. Finally, the results of the formulated optimization problems are presented to illustrate the economic advantages of CA and the cognitive bandwidth allocation strategy. The main simulation parameters are listed in Tables II
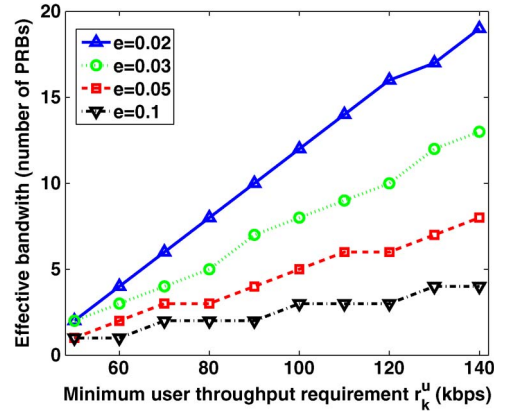

Fig. 5. Effective bandwidth vs. minimum throughput requirement under different e values.

and III, where the effective bandwidth is measured by the number of PRBs per user, i.e., P_k^u.

A. Effective Bandwidth

We first show how the effective bandwidth B_k^u changes with the minimum throughput requirement r_k^u in Fig. 5 via *Monte Carlo* simulations. The parameter values in Table II are used. It can be seen that for all the simulated values of e, B_k^u presents a non-decreasing trend with increasing r_k^u. This is because the system has to spend more bandwidth to guarantee a larger minimum throughput requirement given e and the wireless channel statistics. For each curve, the flat part occurs, because a PRB is the minimum bandwidth allocation unit. Besides, we can observe that the effective bandwidth increases faster with smaller e. This is explained as follows. According to (11), e is positively correlated with r_k^u/B_k^u. Therefore, if r_k^u increases by a fixed ratio, B_k^u has to increase by larger ratio for smaller e, i.e., for smaller e, the slope of the $r_k^u - B_k^u$ curve is larger.

B. Fixed-Weight Strategy

In this subsection, we evaluate the EC performance for the fixed-weight strategy. We first consider single user class to show how the ECs N^{LTE} and N^{LTE-A} vary with different parameters. The class-1 values in Table III are used. Both analytical and simulated results are shown in Fig. 6, where the four evaluated parameters are loss probability δ_1, the number of assigned PRBs P_k^u, the number of aggregated CCs n, and active probability p_1. We have the following observations.

i) The simulated results agree well with the analytical ones for both LTE-A and LTE users under all simulated parameters, except when the loss probability is higher than 0.01 in Fig. 6(a). The reason is that when the loss probability is very high (e.g., larger than 0.01), the third item of (20) becomes non-negligible since z is very close to or even lower than 3, making the approximation inaccurate.

ii) For all the subfigures, the ECs of LTE-A users surpass those of LTE users significantly except in the zero-gain situations. The gain (i.e., the ratio of ECs between LTE-A and LTE users) comes from the semi-usage PRBs mentioned in Section III-A. Although these PRBs only account for a very small portion of the whole transmission
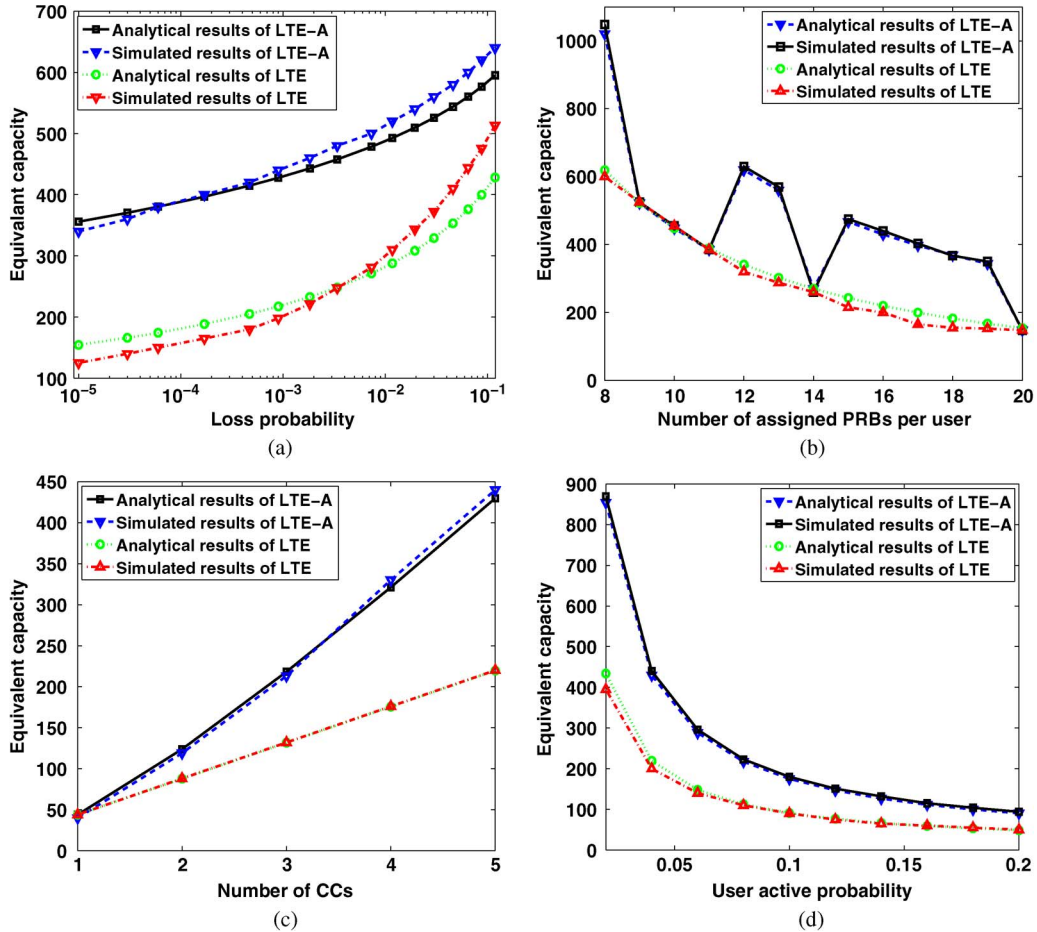
Fig. 6. Fixed-weight strategy: ECs under 4 different parameters (default values: $p_1 = 0.04$, $n = 5$, $P_1^u = 16$, $\delta_1 = 10^{-3}$). (a) User loss probability; (b) assigned bandwidth per user; (c) number of CCs; (d) user active probability.

bandwidth, i.e., the spectrum utilization of LTE-A users is only $2.5\% \sim 16\%$ higher than that of LTE users in Fig. 6, the achieved EC gain can be as high as around 2. The notable gain can be explained as follows. Recall (26) and (27), due to the introduction of δ_k, EC increases nonlinearly and faster when the normalized bandwidth increases. Take the default settings of Fig. 6 as an intuitive example: The 5 CCs can concurrently serve at most 30 LTE users or 31 LTE-A users. When there are 31 LTE users in the system, the loss probability is p^{31}. When there are 32 LTE-A users, the loss probability is p^{32}. As $p \ll 1$, p^{32} is much smaller than p^{31}. Hence, many more LTE-A users can be admitted into the system to make the two loss probabilities the same, resulting in a high EC gain.

iii) The gain increases as the number of PRBs per user or the number of aggregated CCs increases (except for the zero-gain situation), but stays unchanged with the active probability. This is because the portion of the semi-usage PRBs becomes larger (except the zero-gain situation) with the increase of the number of PRBs per user or CCs, resulting in a larger spectrum utilization with LTE-A users, while the utilization stays the same for different active probabilities.

iv) The zero-gain situations occur in Fig. 6(b) when the number of assigned PRBs per user is equal to 9–11, 14, or 20.
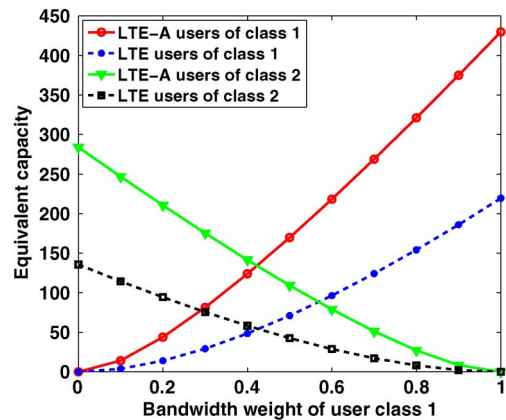

Fig. 7. Fixed-weight strategy: The relationship between the ECs of 2 user classes with changing bandwidth weights.

The reason is as follows. Based on the parameter settings, there are totally 100 PRBs per CC. If we take $P_1^u = 9$ as an example, at most 11 users can be concurrently served in each CC. When $n = 5$, the left 5 PRBs (one from each CC) are still not enough to support one more user cooperatively. As a result, the bandwidth utilization remains the same for LTE and LTE-A users, leading to zero gain.

Besides, a two-user-class case is further simulated to exhibit the relationship between the ECs of two user classes under
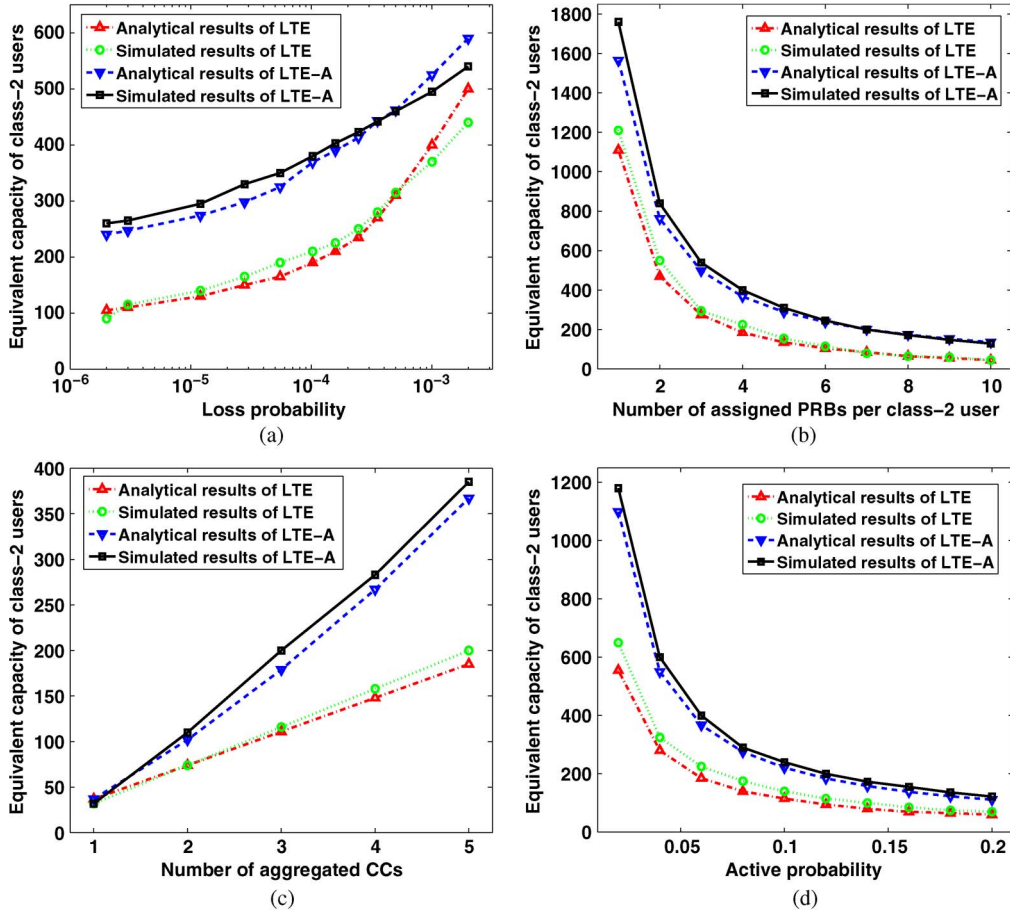
Fig. 8.   Cognitive-weight strategy: ECs of class-2 users under different parameters. (a) User loss probability; (b) assigned bandwidth per user; (c) number of CCs; (d) user active probability.

different bandwidth weights, as shown in Fig. 7, where LTE and LTE-A users are considered, respectively. The default parameter values of class 1 are the same as the above single-class case; and those of class 2, i.e., P_2^u, p_2, and δ_2 are set to be 15, 0.06, and 10^{-4}, respectively. From Fig. 7, we can observe that the ECs of the two classes present a strong negative correlation and either achieves the maximum when assigned with the whole transmission bandwidth.

C. Cognitive-Weight Strategy

In this subsection, we evaluate the EC performance for the cognitive-weight strategy with two user classes. As the main difference from the previous strategy is the EC of the lower-priority user class (i.e., class 2), we only present the ECs of class-2 users with different changing parameters. As shown in Figs. 8 and 9, both analytical and simulated results are given under the parameters in Table III. The default settings are: 1) $\delta_1 = 10^{-4}$, $\delta_2 = 10^{-3}$, $P_1^u = 7$, $P_2^u = 5$, $n = 4$, $p_1 = 0.02$, and $p_2 = 0.06$; 2) $\omega_{l1}^{\max} = 0.8$ and the actually admitted number of class-1 users N_{l1}^{ad} is set to be 90% of the EC N_{l1}.

First, it can be observed that the analytical and simulated results match well in both Figs. 8 and 9 except two cases: when the loss probability is larger than 10^{-3} (Fig. 8(a)) and when $\omega_{l1}^{\max}$ is less than 0.3 (Fig. 9). These relatively large gaps are expected and can be explained with the similar reason as in
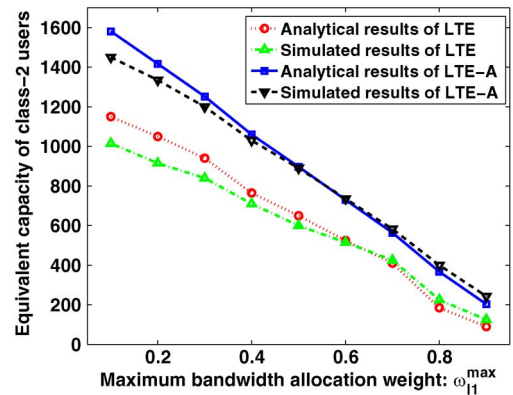

Fig. 9.   Cognitive-weight strategy: theoretical vs. simulated results with changing $\omega_{l1}^{\max}$.

the fixed-weight strategy: when $\delta_2 > 10^{-3}$ or $\omega_{l1}^{\max} < 0.3$, the condition that z_2 in (39) should be larger than 3 cannot hold, and thus our approximation method becomes inaccurate.

Besides, the EC gain of the class-2 LTE-A users over the LTE users increases when the number of CCs, the number of assigned PRBs per user or $\omega_{l1}^{\max}$ increases, while stays almost unchanged with the active probability. This can be explained with the same reason as in the fixed-weight strategy in terms of bandwidth utilization. Moreover, no zero-gain situations occur in Fig. 8(b) when P_2^u changes. This is because for cognitive-weight strategy, the conditions for the zero-gain situation are
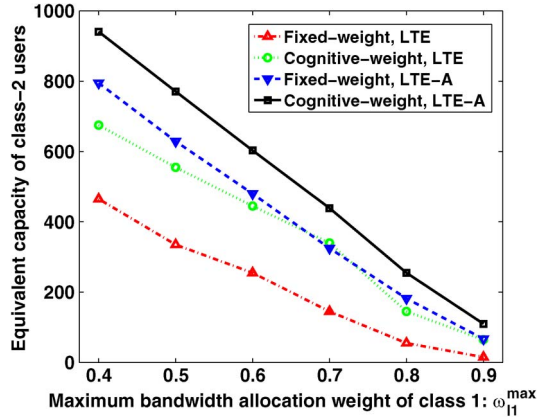
Fig. 10.　EC comparison between fixed-weight and cognitive-weight strategies.
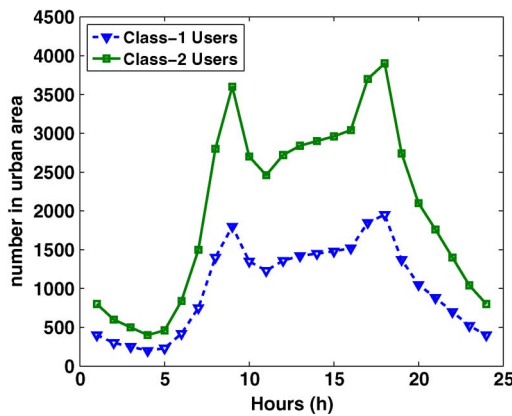

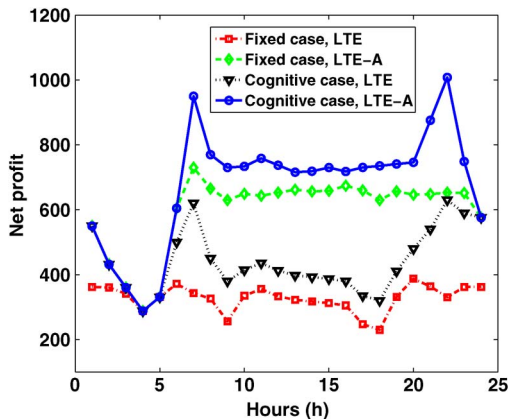Fig. 11.　Annual average hourly number of users per cell in the tested cell.

Fig. 12.　Net profits comparison between fixed-weight and cognitive-weight strategies.

much harder to achieve since the parameters of both user classes are involved therein, as indicated in (45).

D. Performance Comparison Between Two Bandwidth Allocation Strategies

The performance comparisons between the above two strategies in terms of EC and the achieved normalized operator profits are shown in Figs. 10–12, respectively. The parameter values in Table III are used with the same default settings as Section VII-C except that $n = 5$.

Fig. 10 shows how class-2 ECs under different strategies change with the allocation weight of class-1 users. N_{l1}^{ad} is set to the full EC N_{l1}. It can be found that the ECs under the cognitive-weight strategy are considerably higher than those under the fixed-weight strategy for both LTE and LTE-A users. For some weight values, the ECs of LTE users under the cognitive-weight strategy are even close to those of LTE-A users under the fixed-weight one. This is because the bandwidth weight of class-2 users under the cognitive-weight strategy can dynamically change in a cognitive manner as the secondary users do in the typical cognitive radio networks. As a result, more class-2 users can be concurrently served on average, and thus larger EC will be obtained under the same loss probability requirement.

Furthermore, we compare the optimal net profits obtained from the utility-maximization problems formulated in Section VI. The scales of the collected annual average hourly traffic in [39] are used to generate the hourly average number of users per cell in Fig. 11. The hourly optimal net profits are presented in Fig. 12. We can observe that the cognitive-weight strategy outperforms the fixed-weight one significantly for most of the time. The gain comes from that the class-2 ECs under the cognitive-weight strategy are larger when both strategies have the same the class-1 ECs. As shown in Fig. 12, for the LTE-A users, when the traffic load is light (e.g., 1–6 A.M.), all the users in the cell can be admitted into the system, thus the net benefits under two strategies are the same. As the traffic load increases (e.g., 6–7 A.M.), the cell under the fixed-weight strategy will be first saturated and the net profits will be affected by the increasing user dissatisfaction from the rejected users. Since the cell in the cognitive-weight strategy has larger EC, the corresponding net profits will be higher. However, when there are too many users in the cell (e.g., 7–9 A.M.), user dissatisfaction will have larger impact on the net profits, thus leading to a profit reduction. The performance of the LTE users can be explained similarly.

VIII. CONCLUSION

In this paper, we have studied the EC performance of LTE-A systems with CA for LTE and LTE-A users under two bandwidth allocation strategies. The concept of effective bandwidth has been introduced to map the user throughput requirement into the bandwidth requirement considering the wireless channel statistics. Then, closed-form expressions of EC have been derived with the binomial-normal approximation for both kinds of users under both strategies. We have further formulated a net-profit-maximization problem to investigate the tradeoff among the bandwidth weights for heterogeneous user classes. Finally, extensive simulations have demonstrated the accuracy of our analytical results, and have shown that: i) with only a small increase in the spectrum utilization, LTE-A users can have considerably higher EC than LTE users when the user traffic is bursty; and that ii) the cognitive-weight strategy performs better than the fixed-weight one due to stronger adaptability to the traffic load conditions. For the future work, we will investigate the EC performance of LTE-A systems where users have MIMO capabilities.

REFERENCES

[1] R. A. Khan and A. A. Shaikh, "LTE advanced: Necessities and technological challenges for 4th generation mobile network," *Int. J. Eng. Technol.*, vol. 2, no. 8, pp. 1336–1342, Aug. 2012.

[2] D. Astély *et al.*, "LTE: The evolution of mobile broadband," *IEEE Commun. Mag.*, vol. 47, no. 4, pp. 44–51, Apr. 2009.

[3] N. A. Ali, A.-E. M. Taha, and H. S. Hassanein, "Quaility of service in 3GPP R12 LTE-advanced," *IEEE Commun. Mag.*, vol. 51, no. 8, pp. 103–109, Aug. 2013.

[4] Z. Shen, A. Papasakellariou, J. Montojo, D. Gerstenberger, and F. Xu, "Overview of 3GPP LTE-advanced carrier aggregation for 4G wireless communications," *IEEE Commun. Mag.*, vol. 50, no. 2, pp. 122–130, Feb. 2012.

[5] Snapdragon 800 Processors. [Online]. Available: http://www.qualcomm.com/snapdragon/processors/800

[6] LTE Advanced in Unlicensed Spetrum. [Online]. Available: http://www.qualcomm.com/solutions/wireless-networks/technologies/lte-unlicensed

[7] LTE Direct, Operator Enabled Proximity Services. [Online]. Available: https://www.qualcomm.com/products/lte/direct

[8] M. Wang, H. Liang, R. Zhang, R. Deng, and X. Shen, "Mobility-aware coordinated charging for electric vehicles in VANET-enhanced smart grid," *IEEE J. Sel. Areas Commun.*, vol. 32, no. 7, pp. 1344–1360, Jul. 2014.

[9] M. Wang *et al.*, "Real-time path planning based on hybrid-VANET-enhanced transportation system," *IEEE Trans. Veh. Technol.*, 2014, to be published.

[10] "Evolved universal terrestrial radio access (E-UTRA); Carrier aggregation; Base station (BS) radio transmission and reception (Release 10)," 3rd Generation Partnership Project (3GPP), Sophia Antipolis Cedex, France, 3GPP TR 36.808 v10.0.0, Jun. 2012.

[11] M. Awad, V. Mahinthan, M. Mehrjoo, X. Shen, and J. W. Mark, "A dual-decomposition-based resource allocation for OFDMA networks with imperfect CSI," *IEEE Trans. Veh. Technol.*, vol. 59, no. 5, pp. 2394–2403, Jun. 2010.

[12] J. Mao, G. Xie, J. Gao, and Y. Liu, "Energy efficiency optimization optimization for OFDM-based cognitive radio systems: A water-filling factor aided search method," *IEEE Trans. Wireless Commun.*, vol. 12, no. 5, pp. 2366–2375, May 2013.

[13] M. S. Alam, J. W. Mark, and X. Shen, "Relay selection and resource allocation for multi-user cooperative OFDMA networks," *IEEE Trans. Wireless Commun.*, vol. 12, no. 5, pp. 2193–2205, May 2013.

[14] Y. Wang, K. I. Pedersen, T. B. Sørensen, and P. E. Mogensen, "Carrier load balancing and packet scheduling for multi-carrier systems," *IEEE Trans. Wireless Commun.*, vol. 9, no. 5, pp. 1780–1789, May 2010.

[15] K. I. Pedersen *et al.*, "Carrier aggregation for LTE-advanced: Functionality and performance aspects," *IEEE Commun. Mag.*, vol. 49, no. 6, pp. 89–95, Jun. 2011.

[16] R. Zhang, M. Wang, Z. Zheng, X. Shen, and L. Xie, "Cross-layer carrier selection and power control for LTE-A uplink with carrier aggregation," in *Proc. IEEE Globecom*, Atlanta, GA, USA, Dec. 2013, pp. 4668–4673.

[17] L. G. U. Garcia, I. Z. Kovcs, K. I. Pedersen, G. W. O. Costa, and P. E. Mogensen, "Autonomous component carrier selection for 4G femtocells—A fresh look at an old problem," *IEEE J. Sel. Areas Commun.*, vol. 30, no. 3, pp. 525–537, Apr. 2012.

[18] R. Guérin, H. Ahmadi, and M. Naghshineh, "Equivalent capacity and its application to bandwidth allocation in high-speed networks," *IEEE J. Sel. Areas Commun.*, vol. 9, no. 7, pp. 968–981, Sep. 1991.

[19] D. Wu and R. Negi, "Effective capacity: A wireless link model for support of quality of service," *IEEE Trans. Wireless Commun.*, vol. 2, no. 4, pp. 630–643, Jul. 2003.

[20] D. López-Pérez, X. Chu, A. V. Vasilakos, and H. Claussen, "On distributed and coordinated resource allocation for interference mitigation in self-organizing LTE networks," *IEEE Trans. Netw.*, vol. 21, no. 4, pp. 1145–1158, Aug. 2013.

[21] J. Brown and J. Y. Khan, "Key performance aspects of an LTE FDD based smart grid communications network," *Comput. Commun.*, vol. 36, no. 5, pp. 551–561, Mar. 2013.

[22] K. I. Pedersen *et al.*, "An overview of downlink radio resource management for UTRAN long-term evolution," *IEEE Commun. Mag.*, vol. 47, no. 7, pp. 86–93, Jul. 2009.

[23] R. Zhang, Z. Zheng, M. Wang, X. Shen, and L. Xie, "Equivalent capacity analysis of LTE-advanced systems with carrier aggregation," in *Proc. IEEE ICC*, Budapest, Hungary, Jun. 2013, pp. 6118–6122.

[24] A. I. Elwalid and D. Mitra, "Effective bandwidth of general Markovian traffic sources and admission control of high speed networks," *IEEE Trans. Netw.*, vol. 1, no. 3, pp. 329–343, Jun. 1993.

[25] C. Chang and J. A. Thomas, "Effective bandwidth in high-speed digital networks," *IEEE J. Sel. Areas Commun.*, vol. 13, no. 6, pp. 1091–1100, Aug. 1995.

[26] A. Abdrabou and W. Zhuang, "Probabilistic delay control and road side unit placement for vehicular Ad Hoc networks with disrupted connectivity," *IEEE J. Sel. Areas Commun.*, vol. 29, no. 1, pp. 129–139, Jan. 2011.

[27] R. E. Miles, "On the homogeneous planar Poisson point process," *Math. Biosci.*, vol. 6, pp. 85–127, 1970.

[28] F. Aurenhammer, "Voronoi diagrams—A survey of a fundamental geometric data structure," *ACM Comput. Surveys*, vol. 23, no. 3, pp. 345–405, Sep. 1991.

[29] "Base station (BS) Radio transmission and reception (Release 9)," 3rd Generation Partnership Project (3GPP), Sophia Antipolis Cedex, France, 3GPP TS 36.104 v9.1.0, Sep. 2009.

[30] G. Yuan, X. Zhang, W. Wang, and Y. Yang, "Carrier aggregation for LTE-advanced mobile communication systems," *IEEE Commun. Mag.*, vol. 48, no. 2, pp. 88–93, Feb. 2010.

[31] P. T. Brady, "A model for generating on-off speech patterns in two-way conversations," *Bell Syst. Tech. J.*, vol. 48, no. 7, pp. 2445–2472, Sep. 1969.

[32] B. Maglaris, D. Anastassiou, P. Sen, G. Karlsson, and J. D. Robbins, "Performance models of statistical multiplexing in packet video communications," *IEEE Trans. Commun.*, vol. 36, no. 7, pp. 834–844, Jul. 1988.

[33] R. Zhang, M. Wang, Z. Zheng, X. Shen, and L. Xie, "Stochastic geometric performance analysis for carrier aggregation in LTE-A systems," in *Proc. IEEE ICC*, Sydney, NSW, Australia, Jun. 2014, pp. 5777–5782.

[34] M. Haenggi, J. G. Andrews, F. Baccelli, O. Dousse, and M. Franceschetti, "Stochastic geometry and random graphs for the analysis and design of wireless networks," *IEEE J. Sel. Areas Commun.*, vol. 27, no. 7, pp. 1029–1046, Sep. 2009.

[35] B. Błaszczyszyn, M. K. Karray, and H.-P. Keeler, "Using poisson processes to model lattice cellular networks," in *Proc. IEEE INFOCOM*, Turin, Italy, Apr. 2013, pp. 773–781.

[36] M. Schwartz, *Broadband Integrated Networks*, vol. 19. Englewood Cliffs, NJ, USA: Prentice-Hall, 1996, pp. 26–29 and 126–140.

[37] G. E. P. Box, J. S. Hunter, and W. G. Hunter, *Statistics for Experimenters: Design, Innovation, Discovery*, 2nd ed. Hoboken, NJ, USA: Wiley, 2005, p. 130.

[38] S. L. S. Jacoby, J. S. Kowalik, and J. T. Pizzo, *Iterative Methods for Nonlinear Optimization Problems*, Prentice-Hall Series in Automatic Computation. Englewood Cliffs, NJ, USA: Prentice-Hall, 1972, pp. 10–100.

[39] O. Järv, R. Ahas, E. Saluveer, B. Derudder, and F. Witlox, "Mobile phones in a traffic flow: A gegographical perspective to evening rush hour traffic analysis using call detail records," *PLoS ONE*, vol. 7, no. 11, pp. 1–11, Nov. 2012.

Ran Zhang (S'13) received the B.E. degree in electronics engineering from Tsinghua University, Beijing, China, in 2010. He is currently pursuing the Ph.D. degree with the Broadband Communication Research Group, University of Waterloo, Waterloo, ON, Canada. His current research interest includes resource management in heterogeneous networks (HetNets), carrier aggregation (CA) in Long Term Evolution—Advanced (LTE-A) systems, wireless green networks and electrical vehicle charging control in smart grids.

Zhongming Zheng (S'08) received the B.Eng. and the M.Sc. degrees from City University of Hong Kong, Kowloon, Hongkong, in 2007 and 2010, respectively. Currently, he is pursuing the Ph.D degree in electrical and computer engineering with the University of Waterloo, Waterloo, ON, Canada. His research interests include green wireless communication, smart grid and wireless sensor networks.
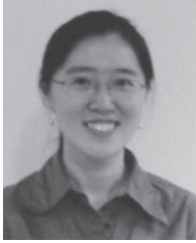
Miao Wang (S'13) received the B.Sc. degree from Beijing University of Posts and Telecommunications, Beijing, China, and the M.Sc. degree from Beihang University, Beijing, China, in 2007 and 2010, respectively. She is currently working toward the Ph.D. degree with the Department of Electrical and Computer Engineering, University of Waterloo, Waterloo, ON, Canada. Her current research interests include the capacity and delay analysis in vehicular networks and electrical vehicle charging control in smart grids.

Xuemin (Sherman) Shen (M'97–SM'02–F'09) received the B.Sc. degree from Dalian Maritime University, Dalian, China, in 1982, and the M.Sc. and Ph.D. degrees from Rutgers University, Camden, NJ, USA, in 1987 and 1990, respectively, all in electrical engineering. From 2004 to 2008, he was the Associate Chair for Graduate Studies and currently, he is a Professor and University Research Chair, Department of Electrical and Computer Engineering, University of Waterloo, Waterloo, ON, Canada. His research focuses on resource management in interconnected wireless/wired networks, wireless network security, social networks, smart grid, and vehicular *ad hoc* and sensor networks. He is a co-author/editor of 12 books and has published more than 700 papers and book chapters in wireless communications and networks, control and filtering. He is an elected member of the IEEE ComSoc Board of Governors, and the Chair of the Distinguished Lecturers Selection Committee. He served as the Technical Program Committee Chair/Co-Chair for IEEE Infocom14, IEEE VTC10 Fall, the Symposia Chair for IEEE ICC10, the Tutorial Chair for IEEE VTC'11 Spring and IEEE ICC08, the Technical Program Committee Chair for IEEE Globecom'07, the General Co-Chair for Chinacom07 and QShine06, the Chair for IEEE Communications Society Technical Committee on Wireless Communications, and P2P Communications and Networking. He also serves/served as the Editor-in-Chief for *IEEE Network, Peer-to-Peer Networking and Application*, and *IET Communications*; a Founding Area Editor for IEEE TRANSACTIONS ON WIRELESS COMMUNICATIONS; an Associate Editor for IEEE TRANSACTIONS ON VEHICULAR TECHNOLOGY, *Computer Networks*, and *ACM/Wireless Networks*; and the Guest Editor for the IEEE JOURNAL ON SELECTED AREAS IN COMMUNICATIONS, *IEEE Wireless Communications, IEEE Communications Magazine*, and *ACM Mobile Networks and Applications*. He received the Excellent Graduate Supervision Award in 2006 and the Outstanding Performance Award in 2004, 2007 and 2010 from the University of Waterloo, the Premiers Research Excellence Award (PREA) in 2003 from the Province of Ontario, Canada, and the Distinguished Performance Award in 2002 and 2007 from the Faculty of Engineering, University of Waterloo. He is a registered Professional Engineer of Ontario, Canada, an Engineering Institute of Canada Fellow, a Canadian Academy of Engineering Fellow, and a Distinguished Lecturer of the IEEE Vehicular Technology Society and Communications Society.

Liang-Liang Xie (M'03–SM'09) received the B.S. degree in mathematics from Shandong University, Jinan, China, in 1995 and the Ph.D. degree in control theory from the Chinese Academy of Sciences, Beijing, China, in 1999.

He did postdoctoral research with the Automatic Control Group, Linkoping University, Linkoping, Sweden, during 1999–2000 and with the Coordinated Science Laboratory, University of Illinois at Urbana-Champaign, Urbana, IL, USA, during 2000–2002. He is currently a Professor in the Department of Electrical and Computer Engineering, University of Waterloo, Waterloo, ON, Canada. His research interests include wireless networks, information theory, adaptive control, and system identification.